JOINT INSTITUTE FOR AERONAUTICS AND ACOUSTICS

NASA
National Aeronautics and
Space Administration
Ames Research Center

NASA-TM-84825 19820021391

Stanford University

JIAA TR - 44

AERODYNAMICS OF AN AIRFOIL WITH A JET ISSUING FROM ITS SURFACE

D.A. Tavella and K. Karamcheti

STANFORD UNIVERSITY
Department of Aeronautics and Astronautics
Stanford, California 94305

MAY 1982

JIAA TR - 44

AERODYNAMICS OF AN AIRFOIL WITH A JET ISSUING FROM ITS SURFACE

D. A. Tavella and K. Karamcheti

The work here presented has been supported by the National Aeronautics and Space Administration under Grant No. NASA NCC 2-74.

ABSTRACT

A simple, two-dimensional, incompressible and inviscid model for the problem posed by a two-dimensional wing with a jet issuing from its lower surface is considered and a parametric analysis is carried out to observe how the aerodynamic characteristics depend on the different parameters. The mathematical problem constitutes a boundary value problem where the position of part of the boundary is not known a priori. A non-linear optimization approach is used to solve the problem, and the analysis reveals interesting characteristics that may help to better understand the physics involved in more complex situations in connection with high-lift systems.

ACKNOWLEDGEMENTS

This research was carried out as a part of the aeronautics program of the Joint Institute for Aeronautics and Acoustics at Stanford University and was sponsored by NASA Ames Research Center. The authors wish to thank Dr. Walter Murray of the Operations Research Department at Stanford University for his helpful advice and discussions.

NOMENCLATURE

SYMBOL	QUANTITY	DIMENSION
c	Chord of airfoil.	L
C^3	Class of function with continuous second derivatives.	0
$\tilde{C}_j$	Momentum coefficient of the jet.	L
C_j	Momentum coefficient of the jet non-dimensionalized with the chord.	0
$F(q)$	Objective function.	0
$G(s), H(s)$	Weight functions.	0
G_i, H_i	Weight factors.	0
J	Momentum flux of the jet.	MT^{-2}
$\mathbf{J}$	Average momentum flux tensor of the jet.	$ML^{-1}T^{-2}$
L	Lift.	MLT^{-2}
L_i	Induced lift.	MLT^{-2}
$\tilde{L}_t$	Truncation length.	L
L_t	Truncation length non-dimensionalized with the chord.	0
P^3	Class of third degree polynomials.	0
p_1 p_2	Pressure on sides (1), (2) of the jet.	$ML^{-1}T^{-2}$
p_∞	Pressure in the free stream.	$ML^{-1}T^{-2}$

SYMBOL	QUANTITY	DIMENSION
Q_i	Intensity of the source ith panel.	$L\ T^{-1}$
q	Independent variable in the optimization process, non-dimensionalized with the chord.	0
R_c	Radius of rounding of internal corner.	L
R	Radius of curvature of the jet.	L
s	Natural coordinate along the boundary.	L
$\bar{U}_\infty$	Velocity of the uniform stream.	LT^{-1}
$\bar{v}_j$	Velocity of the jet fluid.	LT^{-1}
v	Average jet speed.	LT^{-1}
$\bar{u}$	Velocity of the flow field.	LT^{-1}
β	Jet angle with respect the chord.	0
δ	Jet thickness.	L
$\Delta \ell_i$	Non-dimensional length of ith panel.	0
ϕ	Velocity potential of the field induced by the singularities.	$L^2\ T^{-1}$
ρ_j	Density of the jet fluid.	ML^{-3}
ρ	Density of the free flow.	ML^{-3}
$\rho_j \bar{v}_j \bar{v}_j$	Momentum flux tensor of the jet.	$ML^{-1}T^{-2}$

CONTENTS

ABSTRACT . . . . . .

ACKNOWLEDGEMENTS . . . . . .

NOMENCLATURE . . . . . .

Chapter page

I. INTRODUCTION 1

II. THE MODEL AND THE MATHEMATICAL PROBLEM 10

MATHEMATICAL MODEL 10
MATHEMATICAL PROBLEM 15

III. SOLUTION PROCEDURE 17

FINITE WAKE REFORMULATION 17
SPLINE INTERPOLATION 19
FINITE WAKE PROBLEM WITH APPROXIMATE CONTOUR . . 20
THE NON-LINEAR OPTIMIZATION APPROACH 22
Solution of the Boundary Value Problem . . . 23
Solution of the Minimization Problem 24
Direction of Search 25
Univariate Search 27

IV. IMPLEMENTATION OF THE METHOD 28

DEFINITION OF F(q) 28
INDEPENDENT VARIABLES AND PANEL SPACING 29
TRUNCATION LENGTH 31
FREE-STREAMLINES 32
Mathematical Properties 32
Computation of Free-streamlines 33
JET TRAJECTORIES 34
Mathematical Properties 34
The Jet Shape Close to the Exit 35
Shape of the Jet at Infinity 37
COMPARISON WITH ANALYTICAL RESULTS 37

V. THE AIRFOIL-JET-FREESTREAMLINE PROBLEM 40

COMPUTATIONAL MODEL 40

PANEL DISTRIBUTION, INDEPENDENT VARIABLES,WAKE LENGTH 41
THE PARAMETRIC ANALYSIS 43
Initial Guess 43
Local Minima 44
Characteristics of the Optimization Problem . 45
COMPUTATION OF THE AERODYNAMIC COEFFICIENTS . . 46
ACCURACY CONSIDERATIONS 47
EFFECT OF THE DEFINITION OF F(q) 47
EFFECT OF THE IMPLEMENTATION OF THE PANEL METHOD 50
Rounding of Internal Corners 50
Effect of Density of Panels 51
EFFECT OF THE JET PARAMETERS 52

VI. ANALYSIS OF THE RESULTS 54

RELATED SYSTEMS 54
WAKE SHAPE AND VELOCITY DISTRIBUTION 55
AERODYNAMIC COEFFICIENTS AND CENTER OF PRESSURE 56
Jet at 100 % of the Chord 56
Jet at Other Locations on the Chord 57
EFFECTIVENESS OF THE JET 58
LINEARITY 59

VII. CONCLUSIONS AND RECOMENDATIONS 60

CONCLUSIONS 60
Physics Revealed by the Inviscid Model . . . 60
Characteristics of the Method of Solution . . 61
RECOMENDATIONS 62
The Physical Problem 62
The Mathematical Model 62
Improvements on The Method of Solution . . . 63

REFERENCES 82

LIST OF FIGURES

Figure		page
1.	Jet Flap	2
2.	Augmentor Wing	3
3.	Propulsion Wing	4
4.	Wake in Airfoil with a Jet	5
5.	Simplified Inviscid Model	5
6.	Thin Jet	11
7.	Thin Jet Analysis	12
8.	Flow Field due to Entrainment	15
9.	Mathematical Model	16
10.	Finite Wake Contour	18
11.	Spline Function	20
12.	Approximate Contour	21
13.	Truncated Contour for B.V. Problem	23
14.	Source Panels on the Boundary	24
15.	Geometrical Data in F(q)	29
16.	Panel Distribution	30
17.	Truncation Length	31
18.	Computed Free-streamlines	33
19.	Jet Exit Region	34
20.	Two Dimensional Jet into a Uniform Stream	35
21.	Calculated Jet Trayectories	39
22.	Comparison with Analytical Calculation	39

23. Computational Airfoil 40
24. Computational Model 41
25. Distribution of Panels and Independent Variables . . 42
26. Lift vs. Truncation Length 42
27. Series of Minimization Problems 44
28. Non-physical Solution 44
29. Computation of Aerodynamic Coefficients 47
30. Part of Boundary Used in Computation of F(q) 48
31. Rounding of Internal Corner 50
32. Effect of Radius of Rounding 51
33. Distribution of Panels on Airfoil 52
34. The Minimum of the Objective Function 53
35. Related Systems 65
36. Wake Geometry, Jet at 100% of the Chord 66
37. Wake Geometry, Jet at 100% of the Chord 66
38. Wake Geometry, Jet at 50% of the Chord 67
39. Wake Geometry, Jet at 50% of the Chord 67
40. Velocity Distribution, Jet at 100% of the Chord . . 68
41. Velocity Distribution, Jet at 100% of the Chord . . 69
42. Velocity Distribution, Jet at 50% of the Chord . . . 70
43. Velocity Distribution, Jet at 50% of the Chord . . . 71
44. Induced Lift 72
45. Comparison with the Jet Flap 73
46. Total Lift 74
47. Center of Pressure 75
48. Comparison with the Jet Flap 76
49. Effect of the Jet Position on the Lift 77

50. Effect of the Jet Position on the Center of Pressure 78

51. Jet Effectiveness 79

52. Moment Derivative 80

53. Wake Widening 81

Chapter I

INTRODUCTION

The aerodynamic problems presented by V/STOL aircraft are very complex in nature and in recent years extensive work, both theoretical and experimental has been done in this connection. One of the most important set of such problems is motivated by the aerodynamics of powered lift, a concept that aims at obtaining the very high lift coefficients needed in V/STOL flight.

The objective of this study is to pursue the analysis of a simple inviscid model, originally proposed by Karamcheti and Hu[1], which may help in the understanding of the physics involved in some powered high lift systems. Although there is a great deal of idealization present in this model, it is expected that some of the physical characteristics of real problems will be captured.

Typically, a V/STOL aerodynamic problem includes some formidable source of difficulties such as tridimensionality, non-linearities, separated flows and turbulence-related phenomena such as entrainment. In the present study a two dimensional problem will be dealt with and entrainment will not be considered. However the model does include the non-linearities due to the boundary conditions and a very simple representation of a wake type flow.

In the concept of powered lift, lift is produced by the simultaneous operations of two different mechanisms: induced pressure on the wing and ejection of momentum from the aircraft. Usually jets are arranged in the wing, ejecting momentum in the surrounding medium. Part of that momentum contributes to the lift. At the same time the presence of such jet or jets can act on the wing in such a way as to effectively alter the distribution of pressure around it, thus increasing the lift. This additional lift will be called induced lift. Figure 1 illustrates this idea. Consider a two dimensional wing with a jet issuing from its trailing edge. This system will produce a lift given by:

$$L = J\sin\theta + L_i \qquad 1.1$$

Figure 1: Jet Flap

where Q is the rate of momentum outflow into the surrounding medium.

The different arrangements of jets on the wing, their origin, shape etc, give rise to the very large collection of powered lift systems that has been studied, tested, and in some cases applied to experimental aircrafts. The most thoroughly studied of all such systems is the one shown in Figure 1, known as jet flap . The jet flap is seldom used as shown in Figure 1, rather, configurations are used with physical characteristics strongly related to the jet flap. Such would be the case of the system shown in Figure 2

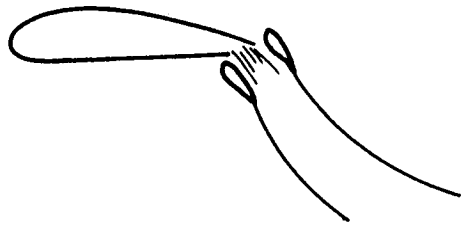

Figure 2: Augmentor Wing

This is known as augmentor wing, where the lift is augmented through entrainment. The augmentor wing is an ejector-type configuration where a thick jet exits at the rear end of the system. Such a thick jet results from the turbulente mixing of the primary thin jet exiting at the trailing edge of the wing with the entrained fluid. Althoug the jet is effectively thick in this case, substantial understanding of the aerodynamics of this system can be arrived at through the analysis of the jet flap shown in Figure 1, used as a simpler model.

The present study concerns itself with furthering the analysis of a model problem which may help in the understanding of the physics of the type of high lift system shown in Figure 3.

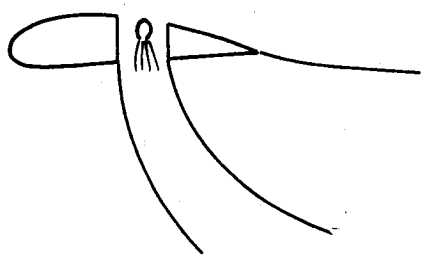

Figure 3: Propulsion Wing

Here the operational principle is the same as the one shown in Figure 2, only that now the ejector is located at a different position on the chord. The flow configuration in this case is expected to be considerably more complicated than in the previous case. In 1972 Galen Hu conducted flow visualization experiments of a configuration somewhat similar to the one shown in Figure 3, but without suction on the upper surface. This system, which is illustrated in Figure 4 according to Hu's experiments, will be the central object of this study and will be refered to as 'the airfoil with a jet' or 'the airfoil-jet- free-streamline problem'.

From Hu's experiments one sees that the jet curves backwards and that there is a vaguely defined wake behind it. Such a wake is turbulent and closed. Experiments also

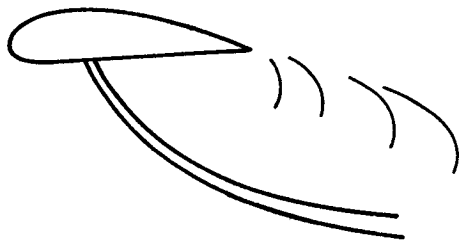

Figure 4: Wake in Airfoil with a Jet

indicate that the pressure inside such a wake is somewhat less than the pressure in the free stream. In Hu's work, the model sketched in Figure 5 was proposed for the study of such a system:

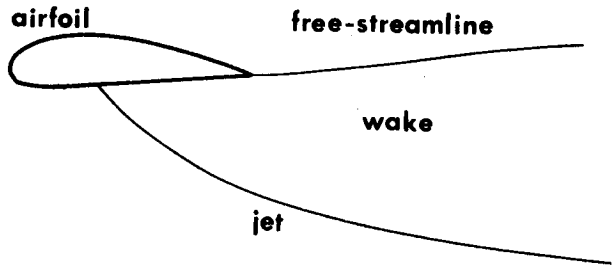

Figure 5: Simplified Inviscid Model

Here the jet is assumed to emerge from the lower surface of the wing. It is also assumed that the jet is infinitely thin, that the flow is incompressible and inviscid and that there is a dead air region enclosed by the jet and a free-stream line starting at the trailing edge. The pressure in the dead air region was assumed to be constant and equal to the pressure in the free stream. This leads to a semi-infinite, open wake.

In the current study this same model will be analyzed further. A more realistic model should take into account the fact that the wake is closed, this however, represents a very great difficulty in the context of an inviscid model. Different alternatives are considered in chapter 2, where some consideration is given to the additional information that would be needed to formulate a closed wake model. Using this infinity wake model, Hu calculated the pressure distribution for different locations and strengths of the jet. The mathematical problem posed by the model consists of solving Laplace's equation in a two-dimensional exterior domain whose boundaries are given by the airfoil, the jet and the free-streamline. If the shapes of the jet and the free-streamline were known, the problem could easily be solved using some appropriate method for solving the Laplace's equation in that particular domain. Those shapes, however, are not known a priori, and they are, in fact, part of the solution. The shape of the free-streamline should be such that the pressure along it be a constant, equal to the pressure in the wake. The shape of the jet should be such that the centrifugal force due to its curvature be balanced by the pressures acting on it.

Hu devised an approximate technique for solving this problem consisting of using the method of singularities to calculate the pressure distribution around the contour and an iterative procedure to find the jet shape. In Hu's

approach the shape of the free-streamline was not actually calculated, but rather it was assumed, drawn with the aid of a french curve, and then incorporated in the problem. The iterative procedure used to estimate the jet shape consisted of replacing the jet shape with connected straight line segments and requiring that the pressure jump between both sides of such segments be balanced at a discrete number of points by the change of direction of the momentum vector of the so represented jet shape. The shape of the jet shape is then iterated upon, until the pressure and momentum change are properly related. During this procedure the free-streamline is assumed to be known and invariant, given by an initial guess that satisfies the condition of tangency at the separation point and behaves suitably at large distances from the wing. Hu points out that, if the initially satisfactory shape of the free-streamline is no longer acceptable after the shape of the jet has been iterated upon, one can repeat the procedure and make another guess for the free-streamline shape. Using this technique, Hu calculated pressure distributions on the airfoil for different jet locations, settings and strengths. However, no aerodynamic coefficients were calculated.

In order to extract as much information as possible from this simple mathematical model it is desirable to carry out a parametric study of the effects on the aerodynamic coefficients of quantities such as jet strength, jet angle

and jet location. This requires the development of a more flexible technique capable of computing the free-streamline and jet shapes simultaneously. In this study such a technique is developed in chapter 3. The basic idea underlying this new procedure is that this boundary value problem can be reformulated as a non-linear optimization problem, in which the objective function is a convex function of parameters characterizing the shapes of the jet and the free-streamline. The minimum of this function will occur for values of the parameters corresponding to approximate jet and free-streamline shapes.

The main difference between the method developed here and the one used by Hu is the fact that the present method is a general one capable of treating a variety of boundary value problems where the position of the boundary is unknown a priori, and it is possible to construct an objective function such that the desired shape of the boundary corresponds to the minimum of the objective function. In this work the formulation of the method is executed in reference to the particular type of cavity, or wake, that the inviscid model for the airfoil with the jet contains. However many of the considerations exemplified in the airfoil-jet-freestreamline problem will be valid in a different class of problems also.

In addition to its generality and greater flexibility, the present technique also shows substantial improvements in computing the boundary shape over Hu's results. Concerning

the jet shape, the improvement comes about through the representation of the jet by cubic splines as opposed to connected straight segments. Concerning the free-streamline, the improvement is due to the much greater accuracy with which the boundary conditions are satisfied there. In fact, a behaviour of the free-streamline shape in response to changes in the jet parameters is exhibited, which wasn't observable in Hu's work.

The parametric study reveals that, for the particular case of the jet located at the trailing edge, the presence of the wake produces a very large loss of induced lift. It is also observed that for a given location of the jet for the wing at zero angle of attack, the position of the center of pressure is chiefly a function of the jet strength only, thus independent of the jet angle. This result happens to hold exacly for the classical linearized analysis of the jet flap. It is also found that there is a remarkably linear relation between quantities such as lift, jet penetration and free-streamline displacement and the angle of the jet, even for rather large values of such angle.

This Page Intentionally Left Blank

Chapter II

THE MODEL AND THE MATHEMATICAL PROBLEM

2.1 MATHEMATICAL MODEL

As explained in chapter 1., the model depicted in Figure 5 will be solved using a new approach and studied parametrically. The following are important properties of the model that will be explained in some detail:

1. The jet is idealized as being an infinitely thin lamina with finite momentum flux and zero mass flux.

This way of representing two-dimensional jets was developed by Spence.[2] Hu followed Spence's development. The following relationship relates the radius of curvature of the jet to the momentum and the pressure difference between across the jet.

$$P_1 - P_2 = \frac{J}{R} \qquad 2.1$$

Here J is the jet momentum flux and R is the radius of curvature of the jet, see Figure 6.

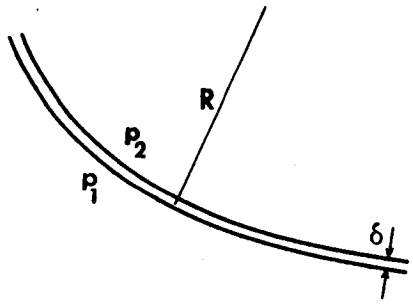

Figure 6: Thin Jet

Spence arrives at this result assuming that the flow within the jet is irrotational and then letting the thickness of the jet go to zero. However, the condition of irrotationality is not necessary for equation 2.1 to apply. In reality the jet is not irrotational, although it may still be thougth to be thin. A simpler derivation of equation 2.1 that does not assume irrotationality goes as follows:

Consider a segment of the jet of length Δs as shown in Figure 7. The equilibrium of forces acting across the jet requires

$$(p_1-p_2)\Delta s\bar{r}_3 = \int \rho_i v_i v_i \bar{n} dA \qquad 2.2$$

where $\rho_i v_i v_i$ is the momentum flux tensor. The average of the momentum flux tensor defined by

$$\bar{J}\cdot\bar{n}\ \delta = \int \rho_i v_i v_i \bar{n} dA \qquad 2.3$$

where the integral is taken over the cross section of the control volume shown in Figure 7. In the coordinate system shown in Figure 7 the average momentum flux tensor is assumed to have the form

$$\bar{\bar{J}} = \begin{bmatrix} J_{11} & 0 \\ 0 & 0 \end{bmatrix} = \begin{bmatrix} \rho_1 v^2 & 0 \\ 0 & 0 \end{bmatrix} \qquad 2.4$$

where v is an average jet velocity. This form of the momentum flux tensor amounts to the assumption that the velocity of the fluid within the jet is essentially normal to the normal cross-section of the jet. The equation of force balance can then be rewritten

$$(p_1 - p_2)\bar{n}_3 \Delta s = \bar{\bar{J}} \cdot \bar{n}_1 \delta + \bar{\bar{J}} \cdot \bar{n}_2 \delta \qquad 2.5$$

since $\bar{n}_1 \; \bar{n}_2 = 2\alpha \bar{n}_3$ and $\alpha = \Delta s / 2R$

$$(p_1 - p_2)\bar{n}_3 \Delta s = J_{11} \delta \frac{\Delta s}{R} \bar{n}_3 \qquad 2.6$$

hence

$$p_1 - p_2 = J_{11} \frac{\delta}{R} \qquad 2.7$$

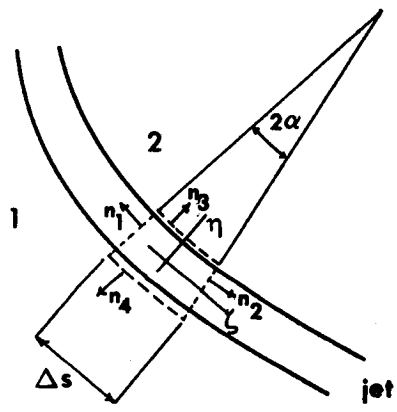

Figure 7: Thin Jet Analysis

Hence, identifying J with $J_{11}\delta$, equation 2.1 is still valid for rotational jets as long as they are sufficiently thin in order that R may be defined as the radius of curvature of its trajectory.

2. The wake is assumed to have constant pressure, equal to the pressure of the free stream, and be bounded by a free-streamline starting at the trailing edge.

This assumption implies a wake of infinite length. The assumption that the free-streamline starts at the trailing edge is supported by photos taken from experiments that led to the sketch shown in Figure 4. In reality the wake is closed and it would be desirable to formulate a mathematical model with a closed wake. This proves to be quite difficult due to the following fact: It was shown by Birkhoff and Zarantonello[3] that "a closed wake with constant pressure lower than the pressure at infinity is mathematically impossible". This is shown to be a property of wakes in inviscid ideal flow. What this fact implies is that if the wake is to be closed the pressure in it cannot be uniform and lower than the pressure of the free-stream. If the pressure is assumed to be less than the free-streamline pressure somewhere in the wake, then it will necessarily have to vary inside the wake if a meaningful solution is to be obtained. This means that formulating a closed wake inviscid model

would require assumptions as to how the pressure varies, to do this a great deal of yet unavalaible experimental data are needed.

If a thin jet is a boundary of a wake with constant pressure equal to the pressure of the free-stream, the jet equation can be expressed in terms of the velocity potential as follows: In the sketch in Figure 7 it is assumed that the wake exists in region 2 and that in region 1 there is a potential flow field consisting of a uniform field of velocity $\bar{U}$ plus a disturbance field of velocity $\nabla\phi$. Bernoulli's equation is

$$p_1 = p_\infty + \frac{1}{2}\rho(U_\infty^2 - (\nabla\phi + \bar{U}_\infty)^2) \qquad 2.8$$

on side 2

$$p_2 = p_\infty \qquad 2.9$$

hence equation 2.1 becomes

$$\frac{1}{2}\rho(U_\infty^2 - (\nabla\phi + \bar{U}_\infty)^2) = J_{11}\delta/R \qquad 2.10$$

Defining the momentum coefficient of the jet by $\bar{C}_j = \frac{J_{11}\delta}{\frac{1}{2}\rho U_\infty^2}$, the jet equation becomes:

$$1 - \frac{(\nabla\phi + \bar{U}_\infty)^2}{U_\infty^2} = \frac{\bar{C}_j}{R} \qquad 2.11$$

3. The model ignores entrainment.

Entrainment has the effect of altering the flow field in a way sketched in Figure 8, where the flow pattern shown is due to entrainment alone. This effect is qualitatevely similar to what would be obtained by distributing sinks along suitably chosen boundaries, this distribution of sinks would give rise to an additional flow field, whose streamlines are sketched in Figure 8. This flow is superposed to the flow free from entrainment, and can pressumably alter the pressure distribution appreciably. Such distribution of sinks to represent entrainment constitutes a standard procedure, but requires experimental results indicating how the turbulent entrainment takes place for each configuration.

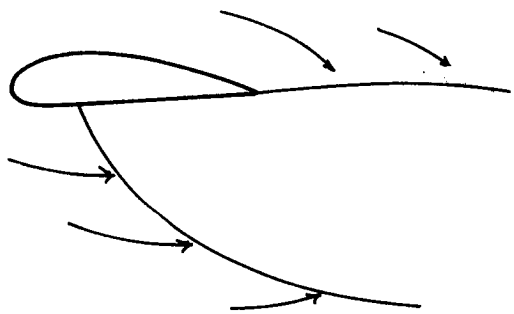

Figure 8: Flow Field due to Entrainment

2.2 MATHEMATICAL PROBLEM

Figure 9 shows the domain where the problem is to be solved.

Defining the velocity at an arbitrary point in Ω to be given by

$$\bar{u} = \nabla\phi + \bar{U}_\infty \qquad 2.12$$

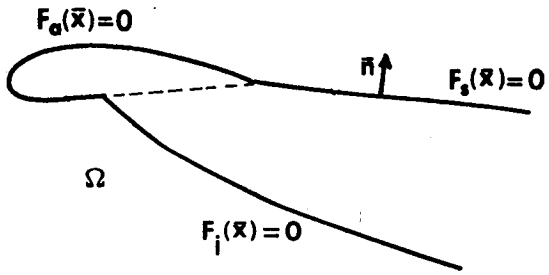

Figure 9: Mathematical Model

the problem consists of solving Laplace's equation

$$\nabla^2\phi = 0 \quad \text{in } \Omega \tag{2.13}$$

subject to the following conditions:

Tangency at the boundary

$$\nabla\phi\,\bar{n} = -\bar{U}_\infty\bar{n} \quad \text{on } F_s(\bar{x})=0\,, \quad F_a(\bar{x})=0\,, F_i(\bar{x})=0 \tag{2.14}$$

Constant pressure on free-streamline

$$|\nabla\phi + \bar{U}_\infty| = |\bar{U}_\infty| \quad \text{on } F_s(\bar{x})=0 \tag{2.15}$$

This equation will also be called the 'free-streamline condition'.

Balance of forces across the jet

$$1 - \frac{|\nabla\phi + \bar{U}_\infty|^2}{U_\infty^2} = \frac{\tilde{C}_j}{R} \tag{2.16}$$

This equation will also be called the 'jet condition'. The method of solution is discussed in the next chapter.

This Page Intentionally Left Blank

Chapter III

SOLUTION PROCEDURE

The method of solution presented in this chapter is of application to a class of boundary value problems of which the airfoil with the jet is a particular example. Among such are problems involving boundaries of cavities bounded free-streamlines, jets or both.

3.1 FINITE WAKE REFORMULATION

The exact mathematical problem described in chapter 2 can be reformulated into one with a finite or truncated wake as shown in Figure 10, where the part of the contour denoted by "C" is assumed to either extend to infinity or to encircle the airfoil at a large distance. Part of the domain in Figure 10a overlaps with the domain Ω in Figure 10b, and so does part of the contour. Figure 10b shows a contour that has a finite wake. The reformulated problem using the contour shown in Figure 10b is then

Laplace's equation

$$\nabla^2\phi = 0 \quad \text{in} \quad \Omega \qquad 3.1$$

Tangency condition

$$\nabla\phi\cdot\bar{n} = -\bar{U}_\infty\cdot\bar{n} \quad \text{on} \quad y = y_s(x) \ , \ F_\alpha(x)=0 \ , \ y = y_j(x) \qquad 3.2$$

Boundary condition on "C"

$$\nabla\phi = \bar{\epsilon}(\bar{x}) \quad \text{on} \quad C \qquad 3.3$$

Free-streamline condition

$$|\nabla\phi + \bar{U}_\infty| = |\bar{U}_\infty| \quad \text{or} \quad y = y_s(x) \qquad 3.4$$

Jet condition

$$1 - \frac{|\nabla\phi + \bar{U}_\infty|^2}{|U_\infty|^2} = \frac{\tilde{C}_j}{R} \quad \text{on} \quad y = y_j(x) \qquad 3.5$$

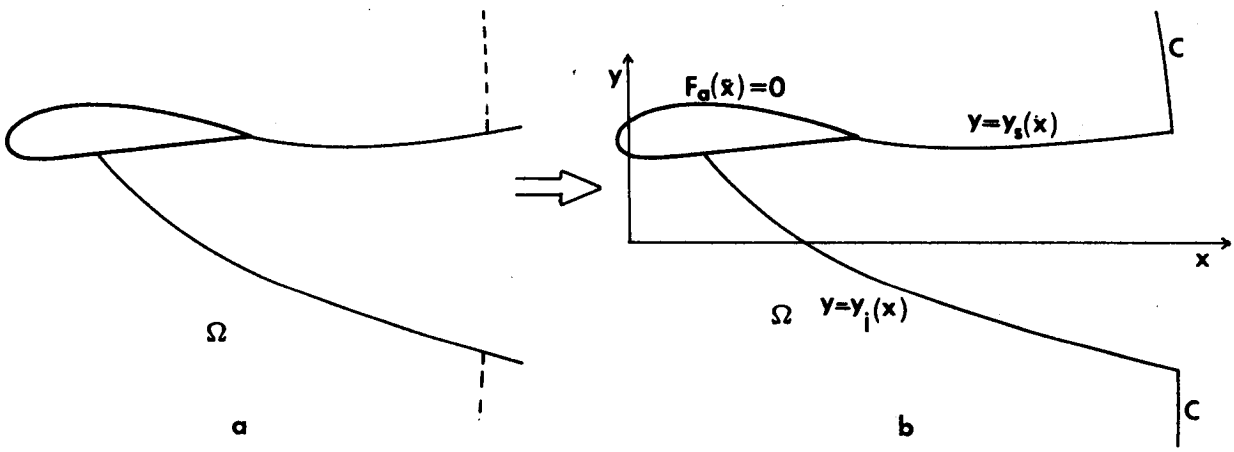

Figure 10: Finite Wake Contour

The function $\bar{\epsilon}(\bar{x})$ in equation 3.3 is taken to be identical to the gradient of the solution of the exact mathematical problem , evaluated at the part of the contour denoted by "C" in the finite wake problem. In this case the solution

of the problem above will be identical to the solution of the exact mathematical problem in the overlapping part of the domains. By virtue of this fact an approximate solution of the so reformulated problem will also provide an approximation to the solution of the exact mathematical problem on the contours that both have in common. The steps that follow show how the construction of such an approximate solution is achieved. Since in this process the spline functions will be used, the concept of spline interpolation will be briefly described first.

3.2 SPLINE INTERPOLATION

A cubic spline function $S(q;x)$ is defined in the following way : given the ordinates q_1 , q_2 , q_n and the slope q_{n+1} define $S(q;x)$ such that

$$S(q;x_0) = y_0 \qquad 3.6$$

$$S(q;x_i) = y_i \qquad 3.7$$

$$\left.\frac{dS(q;x)}{dx}\right]_{x_n} = q_{n+1} \qquad 3.8$$

$$S(q;x) \in C^2 \quad \text{in} \quad [x_0, x_n] \qquad 3.9$$

$$S(q;x) \in p^3(x) \quad \text{in} \quad]x_i, x_{i+1}[\qquad 3.10$$

as shown in Figure 11.

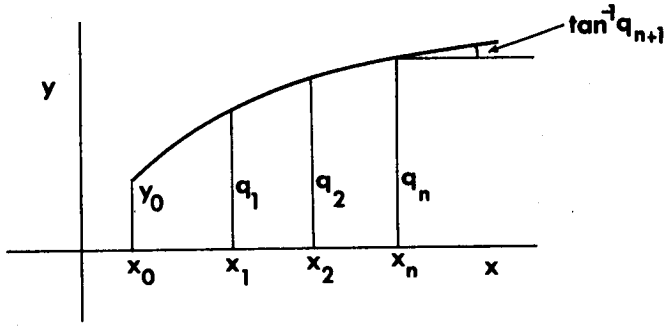

Figure 11: Spline Function

Cubic splines have been studied in great detail and found to have striking convergence characteristics[4]

3.3 FINITE WAKE PROBLEM WITH APPROXIMATE CONTOUR

If spline functions are used to approximate the free-streamline and the jet part of the contour shown in Figure 10b, the problem can be expressed as follows, with the contour described in Figure 12

$$q^s : q_1^s, \ldots, q_{ns+1}^s \qquad 3.11$$

$$q^j : q_1^j, \ldots, q_{nj+1}^j \qquad 3.12$$

$$q : q^j \cup q^s \qquad 3.13$$

$$\nabla^2\phi = 0 \quad \text{in} \quad \Omega \qquad 3.14$$

$$\nabla\phi\cdot\bar{n} = -\bar{U}_\infty\bar{n} \quad \text{on} \quad y = S_s(q^s;x)\ ,\ F_d(x)=0\ ,\ y = S_j(q^j;x) \qquad 3.15$$

$$\nabla\phi = \bar{\epsilon}(\bar{x}) \quad \text{on} \quad C \qquad 3.16$$

$$F(q) \text{ minimum} \qquad 3.17$$

$$F(q) = \left\{ \left\| |\nabla\phi + \bar{U}_\infty| - |\bar{U}_\infty| \right\|_{\text{on } y = S^s(q^s;x)} + \left\| 1 - \frac{|\nabla\phi + \bar{U}_\infty|^2}{U_\infty^2} - \frac{\bar{C}_j}{R} \right\|_{\text{on } y = S^j(q^j;x)} \right\} \qquad 3.18$$

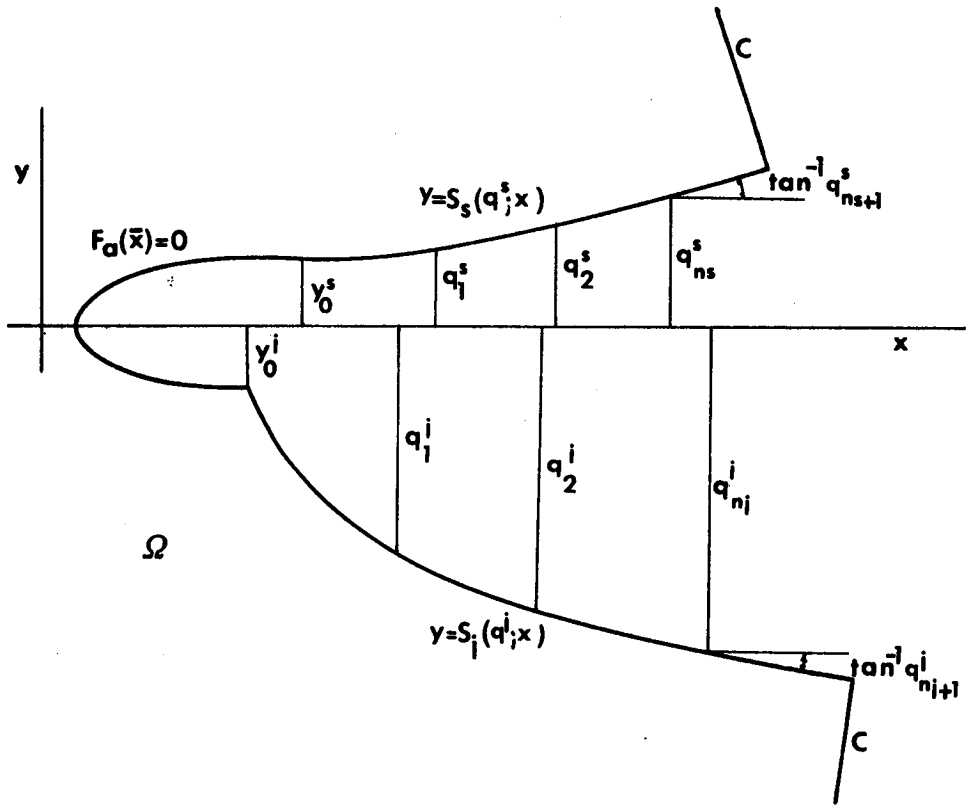

Figure 12: Approximate Contour

In this problem the parameters q characterize the boundary shape and conditions **3.4** and **3.5** have been replaced by the requirement that the function F(q) be minimized. F(q) is constructed adding the norm of the inbalance of the free-streamline condition, eq. 3.4, to the norm of the inbalance of the jet condition, eq. 3.5. These norms will be discussed in detail in chapter 4.

Since the q's characterize the contour, they also characterize the flow field and hence F is a function of q. The rationale behind this approach is that the better y (x) and y (x) in Figure 10b are approximated, the more closely the free-streamline and the jet conditions will be satisfied on the approximate boundary. By taking an accurate enough description of the boundary it should be possible in principle to make F(q) arbitrarily small for the right value of the q's.

3.4 THE NON-LINEAR OPTIMIZATION APPROACH

A crucial step in setting up the problem for solution consists in recognizing the fact that the boundary condition on the "C" part of the boundary can be dropped, namely that the fact that

$$\nabla\phi = \bar{\epsilon}(\bar{x}) \quad \text{on} \quad C \qquad 3.19$$

can be ignored and still an approximate solution to the truncated wake problem can be obtained. The justification for doing so lies mainly in computational experience and on the fact that sufficiently far behind the airfoil the external flow field remains relatively unperturbed. Some of the calculations that will be shown in chapter 4 confirm this assumption. If this is done, the problem can be viewed as follows:

Minimize the function F(q) where the information needed for its evaluation is obtained from the solution of the boundary value problem

$$\nabla^2\phi = 0 \quad \text{in} \quad \Omega \tag{3.20}$$

$$\nabla\phi\cdot\bar{n} = -\bar{U}_\infty\cdot\bar{n} \quad \text{on} \quad \Gamma \tag{3.21}$$

$$\phi \longrightarrow \text{const} \quad \text{at} \infty \tag{3.22}$$

in the domain shown in Figure 13.

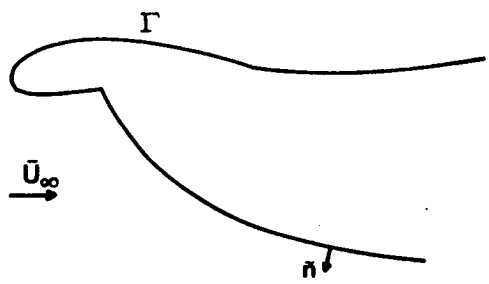

Figure 13: Truncated Contour for B.V. Problem

This constitutes an unconstrained non-linear optimization problem where the objective function is F(q). For each evaluation of the objective function there is a boundary value problem to be solved.

3.4.1 Solution of the Boundary Value Problem

The method used for the solution of the boundary value problem needed in the evaluation of F(q) is the method of singularities using source panels of constant strength distributed on the boundary[5], as shown in Figure 14.

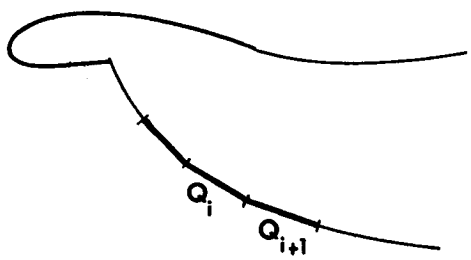

Figure 14: Source Panels on the Boundary

By enforcing the boundary conditions at the center of the panels a set of algebraic equations for the intensities of the sources Q is obtained. Once these are known, the velocity field can be computed at once.

3.4.2 Solution of the Minimization Problem

The task of finding the value of the variables q that minimize the function F(q) is acomplished using a Quasi-Newton algorithm for non-linear unconstrained optimization[6] The optimization procedure is started with an initial estimate of the independent variables q. After this initial estimate is provided, a systematic search in q space is carried out until an approximate estimation of the minimum is reached. A description of the method of minimization will be given next.

The systematic search for the minimum in q space consists of the following steps:

i) If $\bar{q}_k$ denotes the present value of the variables q, a direction of search in q space, denoted by $\bar{p}_k$ is found.

ii) A search along the direction $\bar{p}_k$ is conducted to approximately locate the minimum of F(q) along such direction. The value of q for which that approximate minimum is found is denoted by $\bar{q}_{k+1}$.

iii) Starting at position $\bar{q}_{k+1}$ in q space, steps i and ii are repeated until a satisfactory approximation to the minimum of F(q) is reached. Each sequence of steps i and ii constitutes an iteration.

3.4.2.1 Direction of Search

To illustrate how the direction of search $\bar{p}_k$ in q space is found, consider a quadratic expansion of F(q) about $\bar{q}_k$:

$$F(\bar{q}_k+s) = F(\bar{q}_k) + g_k^T s + \frac{1}{2} s^T G_k s \qquad 3.23$$

where g_k is the gradient of F(q) at $q = \bar{q}_k$ and G_k is the Hessian matrix of F(q) evaluated at $q = \bar{q}_k$. The expression for the quadratic expansion of F(q) has a stationary point at $\bar{q}_{k+1} = \bar{q}_k + \bar{p}_k$ determined by solving the system of equations:

$$G_k \bar{p}_k = -g_k \qquad 3.24$$

This formula provides the direction $\bar{p}_k$ in which a stationary point of the local approximation is to be found. The Quasi-Newton method utilizes a similar formula to determine the direction of search, in which an approximate Hessian is used. An exact expression for the Hessian matrix cannot be

used here because the exact derivatives of the function F(q) are not available.

The approximation to the Hessian matrix at iteration k is denoted by B_k and the direction of search at iteration k is obtained from the solution of the system of equations

$$B_k \, \bar{p}_k = -g_k \qquad 3.25$$

The matrix B_k is updated at each iteration in a way that, as the calculation moves in q space, it acquires progressively more information about the curvature of F(q). At the first iteration the approximation to the Hessian is taken to be the identity matrix,

$$I \, \bar{p}_k = - g_k \qquad 3.26$$

which means that the first direction of search will coincide with the opposite direction of the gradient of F(q) at $\bar{q}_k$. In the first iteration then, the direction of search is the steepest descent direction. To update B_k after the first iteration, the Broyden-Fletcher-Goldfarb-Shanno (BFGS) update formula is used, given by

$$B_{k+1} = B_k - \frac{1}{s_k^T B_k s_k} B_k s_k s_k^T B_k + \frac{1}{y_k^T s_k} y_k y_k^T \qquad 3.27$$

where $s_k = \bar{q}_{k+1} - \bar{q}_k$ an $y_k = g_{k+1} - g_k$. The gradient of F(q) is computed using finite differences. This is believed to be the most effective way of computing the direction of search in the Quasi-Newton method.

3.4.2.2 Univariate Search

Once the direction $\bar{p}_k$ is determined, an approximate minimum of F(q) along it is found. This is acomplished using the so-called safeguarded parabolic interpolation along $\bar{p}_k$, in which the minimum is found within a prescribed accuracy.

This Page Intentionally Left Blank

Chapter IV

IMPLEMENTATION OF THE METHOD

In this chapter the general method described in chapter 3 is applied to free-streamlines and to the problem of a jet issuing from a plane into a uniform stream. For the latter analytical results are available, which are used for comparison with the presente method.

4.1 DEFINITION OF F(Q)

In chapter 3 the objective function F(q) was defined as a norm of the imbalance of the free-streamline condition plus the norm of the imbalance of the jet condition. Refering back to Figure 12, and if the boundary value problem 3.11 to 3.18 were to be solved exacly, a suitable definition for F(q) would be:

$$F(q) = \int_{\text{free-streamline}} H(s)\left(|\nabla\phi + \bar{U}_\infty| - |\bar{U}_\infty| \right)^2 ds + \int_{\text{jet}} G(s)\left(1 - \frac{|\nabla\phi + \bar{U}_\infty|^2}{|U_\infty|^2} - \frac{\tilde{C}_j}{R} \right)^2 ds \qquad 4.1$$

where the integrals in eq. 4.1 are line integrals and G(s) and H(s) are positive weight functions. With this definition F(q) is a smooth function, on which the Quasi-Newton algorithm can be applied.

In implementing the method, a discrete form of eq. 4.1 is used, the objective function is given by:

$$F(q) = \sum_{\text{free-streamline}} H_i \left(|\nabla\phi_i + \bar{U}_\infty| - |\bar{U}_\infty| \right)^2 \Delta\ell_i \quad + \quad \sum_{\text{jet}} G_i \left(1 - \frac{|\nabla\phi_i + \bar{U}_\infty|^2}{|\bar{U}_\infty|^2} - \frac{\tilde{C}_i}{R_i} \right)^2 \Delta\ell_i \quad 4.2$$

where G_i H_i are weight factors, $\nabla\phi_i$ is the gradient of the perturbation potential evaluated at the control point of panel i and R is the radius of curvature of the jet at the absisa of the control point of panel i. The interval $\Delta\ell_i$ is the lenght of panel i, as sketched in Figure 15

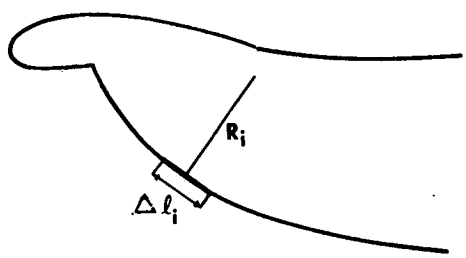

Figure 15: Geometrical Data in F(q)

Weight factors are included in order in order to investigate the flexibility of the definition of F(q).

4.2 INDEPENDENT VARIABLES AND PANEL SPACING

As explained in the previous chapter the variables q are ordinates describing the position of the points of the free-streamline and the jet where the interpolating polynomials match. In order to achieve a good description of the boundary the points characterized by q are taken to be more

closely spaced in parts of the boundary where the curvature is higher. Once the characterization of the boundary through the variables q is established, the panels have to be arranged in a way that changes in the flow field due to 'wiggles' that may exist in the interpolating polynomials be properly captured. This means that a minimum number of panels must exist in between points characterized by the q's. It was found by computational experimentation that there should be at least three panels in between such points. They may or may not be equally spaced. In all the problems dealt with here, the part of the contour that is to be computed is such that its curvature decreases very rapidly downstream, thus allowing for the panels to be much longer in the downstream part of the contour. It was found that a convenient way of distributing the panels is by specifying that their projection on the horizontal axis be given by the expression:

$$\Delta \ell_j \cos\alpha_j = b^{j-1} \Delta \ell_1 \qquad 4.3$$

with b > 1 and j the index characterizing the panel of lenght $\Delta \ell_j$, in the way shown in Figure 16

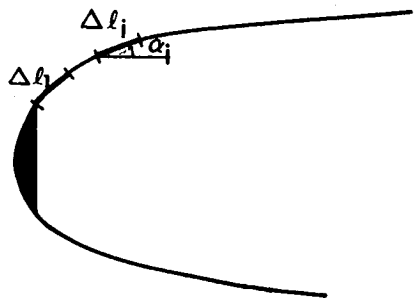

Figure 16: Panel Distribution

This arrangement has the advantage that slight changes in the constant b allow for rather large changes in the lenght of the contour so described keeping the number of panels constant. If the number of panels in between the points on the boundary characterized by the q's is kept constant, eq. 4.3 will also give the distribution of absisae where the q's are specified. This is found to be quite a satisfactory way of describing the contour.

4.3 TRUNCATION LENGTH

The reformulation of the problem with a semi-infinite boundary into one with a finite boundary explained in chapter 3 leads to a problem with a truncated boundary. The overall length of the resultant contour will be called truncation length, as shown in Figure 17

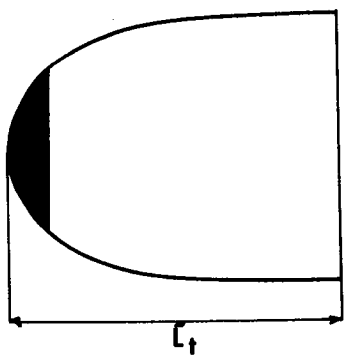

Figure 17: Truncation Length

The interest here is to determine with reasonable accuracy the flow field in the proximity of the body from which jets are ejected or free-streamlines originate. The truncation length has to be chosen in a way that such accuracy is

isured. In this regard each particular problem has to be considered individually.

4.4 FREE-STREAMLINES

4.4.1 Mathematical Properties

The following are properties of free-streamlines given by the mathematical theory of wakes and cavities.

i) Slope at the point of separation: This slope equals the slope of the solid contour from which the free-streamline separates.

ii) Radius of curvature at the point of separation: This radius is equal to infinity or zero, depending on wether the separation point is an inflexion point of the boundary or not. This means that, unless the separation point is an inflexion point, the free-streamline will have singular behaviour at the point of separation.

iii) Behaviour at infinity: Infinitely far downstream, the free-streamline will be paralell to the direction of the velocity of the unperturbed flow field.

4.4.2 Computation of Free-streamlines

A practical example of free-streamline computation using the minimization approach is shown in Figure 18. The free-streamline is assumed to separate at point (a) on the boundary of the semi-infinite barrier. In this case the point of separation is clearly an inflexion point on the boundary, indicating that the curvature of the free-streamline there is zero. In this problem the spline interpolation behaves very well chose to the separation point. With a rather crude distribution of panels the boundary condition for the velocity on the free-streamline is satisfied to within a few per thousand. This example serves as a test for accuracy showing how closely the constant-pressure condition on a free-stremline can be satisfied using the present procedure.

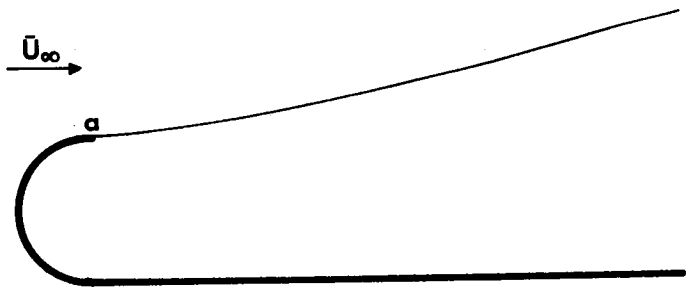

Figure 18: Computed Free-streamline.

4.5 JET TRAJECTORIES

4.5.1 Mathematical Properties

In this section general properties of 2-D infinitely thin jets issuing from bodies inmersed in a uniform stream are pointed out. The description of the jet in the vicinity of its exit and infinitely far downstream should be independent of the particuar shape of the body from which it issues. This idea is illustrated in Figure 19, where, if the jet exit region is magnified, the jet is seen as emerging from a plane.

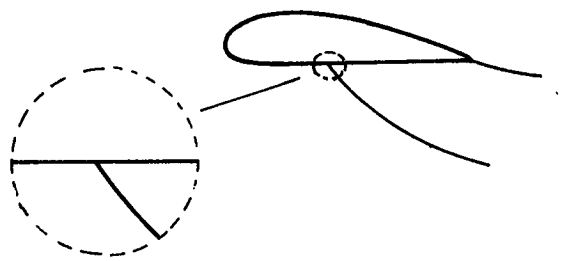

Figure 19: Jet Exit Region

Knowledge of this asymptotic behaviour is of use in the implementation of this method, since it allows one to replace the interpolating polynomials with analytic expressions in regions where the polynomials are likely to behave poorly. Such will be the case of a jet issuing from a horizontal plane normal to a uniform stream. The spline interpolation will behave poorly close to the exit, where the slope of the jet is large, and higher density of variables q would

be needed to improve the behaviour of the interpolation. It will explained later how this, in its turn, would affect adversely the scaling of the objective function. It is then desirable to have an analytic expression for the jet in the neighbourhood of the exit. It is also plausible that in improved versions of this method, the asymptotic behaviour of jets at infinity could be incorporated, by assuming that the jet far downstream has the correct mathematical behaviour, as opposed to the simplified form assumed in this study, as will be shown later.

4.5.1.1 The Jet Shape Close to the Exit

As discussed in Chapter 2 the equation of the jet trajectory is given by

$$p_1 - p_2 = \frac{\tilde{C}_j}{R} \qquad 4.4$$

where $p_1 - p_2$ is the pressure jump across the jet. This quantities are illustrated in Figure 20, picturing a 2-D jet emerging from a slot in a horizontal plane and into a uniform stream.

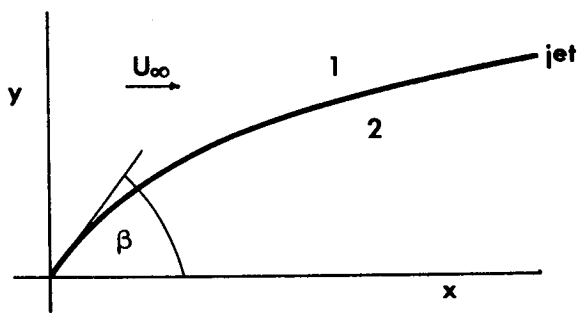

Figure 20: Two Dimensional Jet into a Uniform Stream

If the pressure jump across the jet were known, equation 4.4 could be solved for the trajectory. In general the pressure on side (1) in Figure 20 is a function of the trajectory itself. This is not the case at the exit, where it is physically clear that a stagnation point exists, and the pressure on side (1) of the jet equals the stagnation pressure. This fact allows to integrate equation 4.4 and find an approximate form for the jet valid close to the exit. In terms of the velocity on side (1) of the jet, equation 4.4 can be rewritten:

$$1 - \frac{u^2}{U_\infty^2} = \frac{(1+y'^2)^{3/2}}{y''} \bar{C}_j \qquad 4.5$$

where y denotes the position of the jet. If the exit is located at the origin of coordinates and exits vertically we have that, as $x \to 0$ and $y \to 0$, $u \to 0$ and $y' \to \infty$ and equation 4.5 becomes

$$(y')^3 = y'' \bar{C}_j \qquad 4.6$$

which admits the solution

$$y = \sqrt{2 \bar{C}_j x} \qquad 4.7$$

this being the form of the trajectory very close to the exit. For a jet exiting at an angle β as shown in Figure 20 we have

$$y = x\cot\beta + \bar{C}_j \frac{\cot\beta}{\sin\beta} + \sqrt{2x\bar{C}_j \frac{1+\cot^2\beta}{\sin\beta} + \bar{C}_j^2 \frac{\cot^2\beta}{\sin^2\beta}} \qquad 4.8$$

These expressions for the jet close to the exit can be used to suplement the spline interpolation, which for the case of

very large slopes may not produce a good description of the jet there. From equation 4.5 it is seen that the radius of curvature at the exit is given by

$$R_{exit} = \frac{1}{\bar{C}_j} \qquad 4.9$$

which is of course finite fo all $\bar{C}_j > 0$

4.5.1.2 Shape of the Jet at Infinity

In the airfoil with a jet problem, the information about how the jet behaves far away from the exit can be taken from the problem depicted in Figure 20. The reason for this is that even if the jet is in a different configuration, at sufficiently far away distances from the exit the only disturbance produced on the flow field is due to the jet alone. Ackerberg[7] solved the problem shown in Figure 20 using matched assymptotic expansions and gave the following expression for the jet at infinity

$$\frac{2x}{\bar{C}_j} \cong \left(\frac{2y/\bar{C}_j + \frac{\pi}{2}A^2}{2A}\right)^2 - \frac{1}{2}A^2 \ln\left(\frac{2y/\bar{C}_j + \frac{\pi}{2}A^2}{2A}\right) + O(1) \qquad 4.10$$

$A = \text{const.}$

This behaviour indicates that infinitely far downstream the jet will be infinitely far apart.

4.6 COMPARISON WITH ANALYTICAL RESULTS

The analytical results obtained by Ackerberg[7] for the jet issuing normally into a uniform stream is compared with

the results obtained using the minimization approach. The computations presented next were performed using $\tilde{C}_j = 0.5$. The way the problem was solved was by assuming a refletion of the jet on the plane from which it exits and thus obtaining a symmetric contour. As it was the case with the free-streamline discussed in section 4, a rather crude distribution of panel was used. The panels were assumed to be equally spaced between the q's and the splines were extended to the very end of the contour. Figure 21 shows the trajectories obtained for two different lengths of the resulting truncated symmetric body. It is observed that close to the rear end the jet exhibits the wrong curvature, having an inflection point. This phenomenon is due to end effects and doesn't appear to disturb the shape of the jet at closer distances from the exit. The fact that this occurs can be attributed to the small influece that such a distortion of the jet far downstream exerts close to the exit. This means that the velocity field in the forward part of the jet is not substantially altered by the change in truncation length.

Figure 22 compares the present results with the ones given by Ackerberg. It is seen that, even with a crude distribution of panels there is satisfactory agreament.

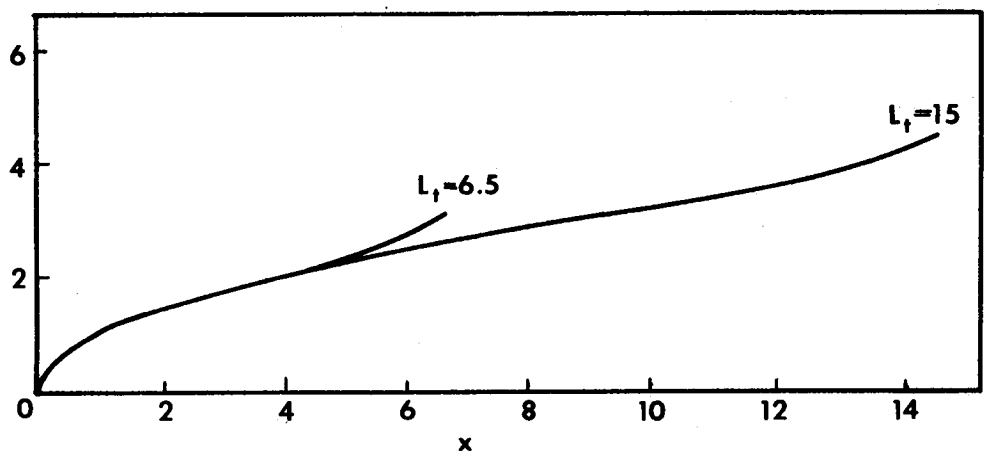

Figure 21: Calculated Jet Trayectories

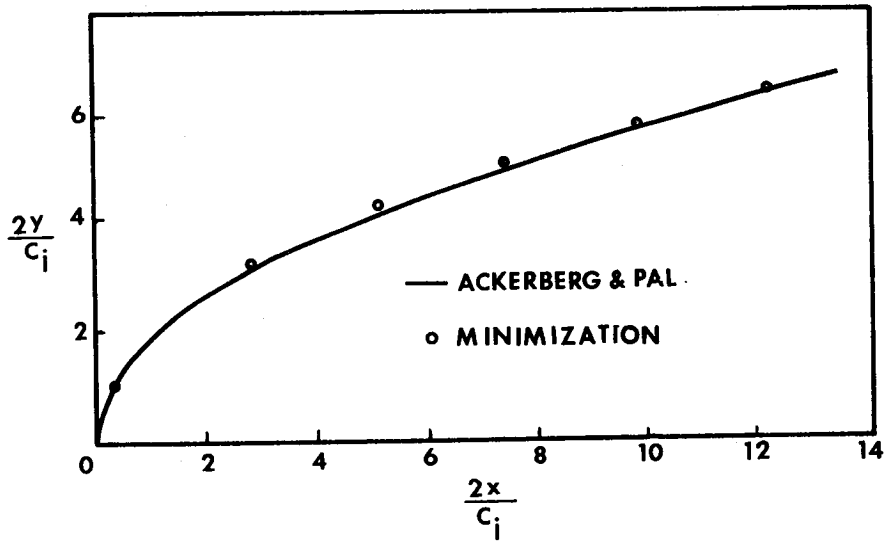

Figure 22: Comparison with Analytical Calculation

Chapter V

THE AIRFOIL-JET-FREESTREAMLINE PROBLEM

In this chapter the method of solution is applied to a computational model. The organization of the parametric study is sketched and considerations regarding accuracy are discussed.

5.1 COMPUTATIONAL MODEL

The main objective of this parametric analysis is to isolate the effects of a few parameters related to the jet and not to the airfoil per se. It is then convenient to use a very simple airfoil with no camber such that only properties related to the jet will be exhibited. Figure 23 shows the airfoil chosen for the calculations. It is a symmetric airfoil with a maximum thickness of 10%, an elliptical nose extending to 25% of the chord and a blunt trailing edge.

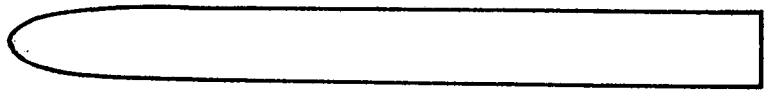

Figure 23: Computational Airfoil

Such an airfoil provides a particularly simple boundary to treat. The fact that it has a blunt trailing edge is of no concern here since no Kutta condition is satisfied in this case. Using this airfoil the problem in question will look as shown in Figure 24

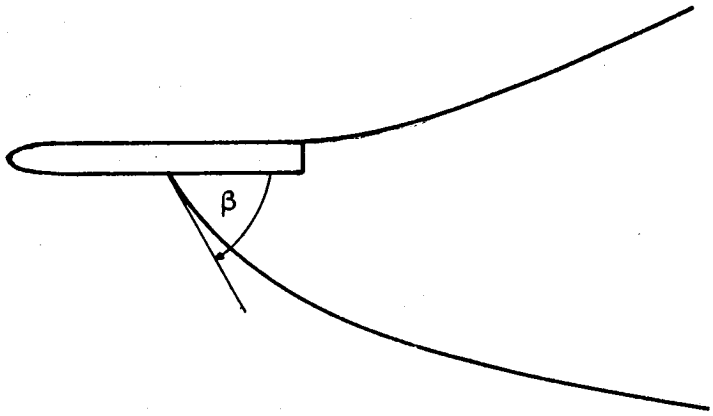

Figure 24: Computational Model

5.2 PANEL DISTRIBUTION, INDEPENDENT VARIABLES, WAKE LENGTH

The panel distribution and the location of the independent variables on the computational model are shown in Figure 25 . On the jet and free-streamline the distribution is laid out according to the description given in section 4.2. A suitable number of panels was found to be about 60, and the total number of independent variables q about 10. The free-streamline has a more easily describable shape, hence the number of independent variables needed to characterize it is lower than the number of independent variables needed to characterize the jet.

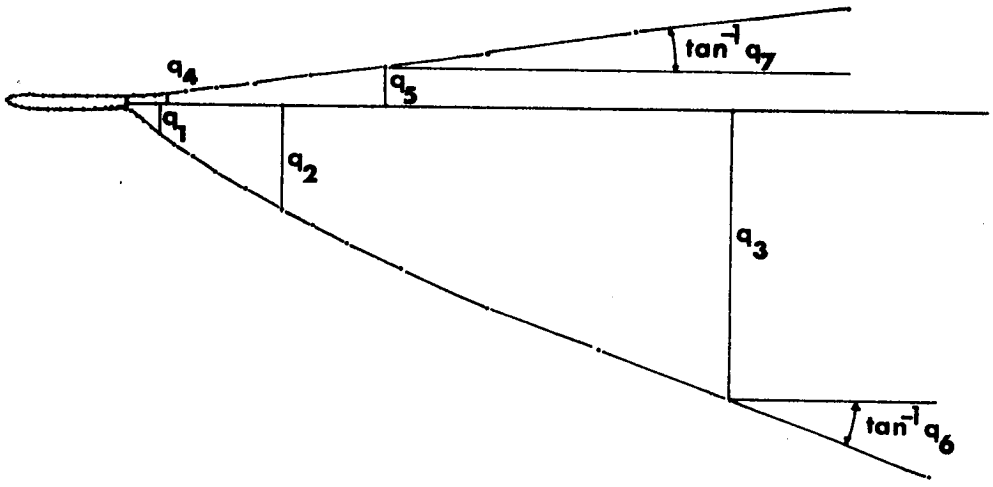

Figure 25: Distribution of Panels and Independent Variables

The truncation length is determined by observing how the aerodynamic coefficients vary as the truncation length varies. Figure 26 shows a typical variation of the lift coefficient as a function of the truncation length measured in multiples of chord length. It is clear from the Figure that beyond a certain length the change in the aerodynamic coefficients is quite small. Such a change is less than one percent when the truncatione length varies between 6 to 10 chord lengths. The length chosen for the parametric analysis is about 8.5 chord lengths.

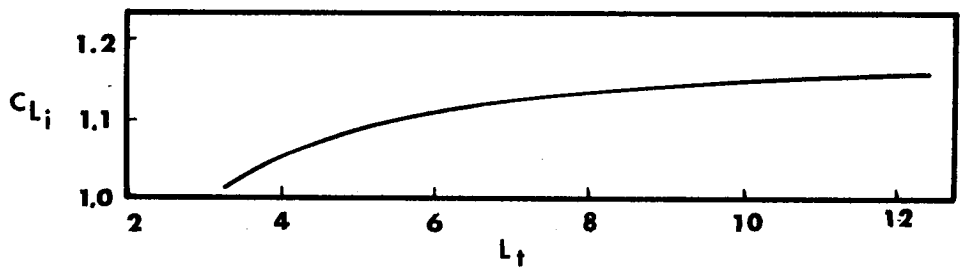

Figure 26: Lift vs. Truncation Length

5.3 THE PARAMETRIC ANALYSIS

5.3.1 Initial Guess

As mentioned in 3.4.2, in order to start the search for the minimum of the objective function an initial estimate of the value of the independent variables at the minimum has to be provided. This amounts to a guess about the shape of the free-streamline and the jet. A first guess for the shape of the free-streamline is to assume that it is a straight line parallel to the airfoil. A first guess for the jet shape can be taken from the trajectory of a jet ejecting from a horizontal plane into a uniform stream as discussed in 4.6.1. With this initial guess for the unknown part of the boundary a series of minimization problems is solved, one for each of the several values of jet strength, jet angle and jet location. The output of each problem serves as initial guess to the next, in the way shown in the following chart.

The motivation for this particular arrangement is that a given relative change in the jet strength produces much less alteration in the shape of the wake that the same relative change in the jet angle. Once the parametric analysis is completed for one position of the jet along the chord, the available results become excellent initial guesses for the jet at different positions. The reason for this is that, all other parameters remaining constant, the geometry of the jet is very slightly modified as a result of changing

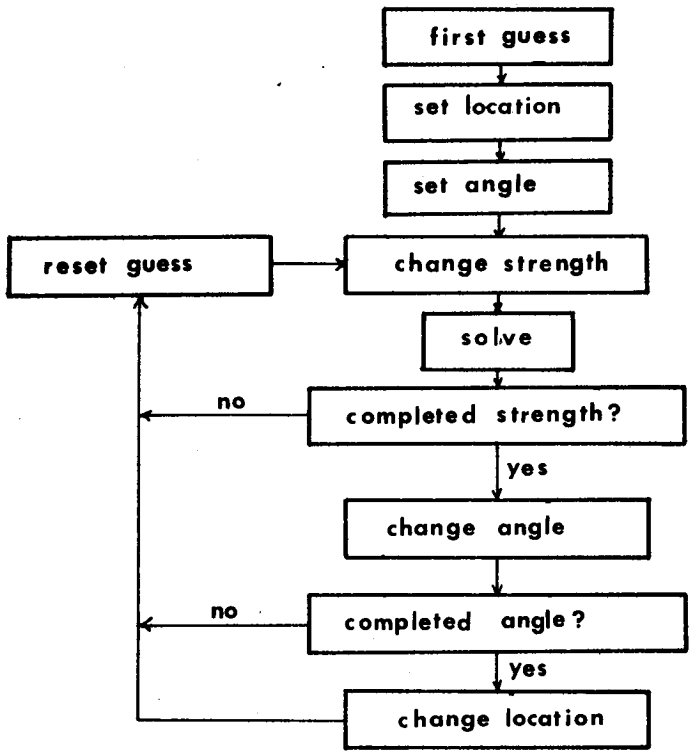

Figure 27: Series of Minimization Problems

the position of the jet exit along the chord, except for the coresponding chordwise translation of the jet shape.

5.3.2 Local Minima

If the initial guess is not reasonably close to the final answer, the procedure may converge to a physically meaningless result. Figure 28 shows such a case.

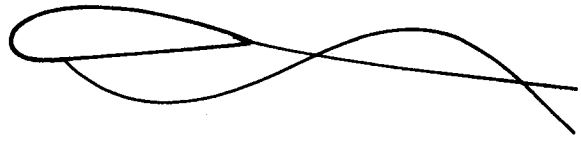

Figure 28: Non-physical Solution

The implication of this fact is that, in general, the minimum of interest is a local one. Non-physical results are readily identifiable since the minimum value of the objective function there is considerably larger than in normal cases. This phenomenon seldom occurs, and it was never observed when the initial guessed where obtained as described in the previous section.

5.3.3 Characteristics of the Optimization Problem

i) Size of the Problem: This is determined by the number of independent variables. A typical such number is 10, which means that the problem is of rather small size.

ii) Cost of Function Evaluation: This is a measure of the amount of computation involved in evaluating the objective function at a given point in q space. In this case this cost is high, of the order of 0.8 sec. of CPU time on the IBM 3033 processor. Lowering this cost would be a considerable improvement on this method, as will be discussed later.

iii) Scaling: A measure of the scaling of an optimization problem is given by the relative magnitude of the different components of the gradient of the objective function and it has considerable importance in the number of iterations needed to reach a solution. In this case the scaling is poor, some components of the gradient being much larger than others.

iv) Typical Number of Iterations: Between 8 and 15.

v) Typical Number of Function Evaluations: Between 70 and 150.

vi) Number of Stationary Points: More than one, however the one of interest is readily identifiable.

5.4 COMPUTATION OF THE AERODYNAMIC COEFFICIENTS

Once the pressure distribution around the airfoil is known, the aerodynamic coefficients are calculated by integrating the pressure coefficient around the airfoil. If the pressure coefficient is defined as

$$C_p = \frac{p - p_\infty}{\frac{1}{2}\rho U_\infty^2} \qquad 5.1$$

The lift coefficient is given by:

$$C_{L_i} = -\frac{1}{c}\int C_p \bar{n}\, ds \qquad 5.2$$

The moment coefficient is given by:

$$C_{m_i} = -\frac{1}{c}\int \frac{\xi}{c} C_p \bar{n}\, ds \qquad 5.3$$

In these formulas the integrals are taken over the surface of the airfoil, as shown in Figure 29

The position of the center of pressure:

$$X_{cp} = c\,\frac{C_m}{C_L} \qquad 5.4$$

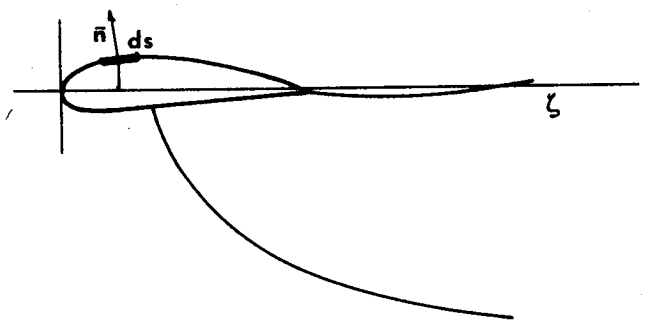

Figure 29: Computation of Aerodynamic Coefficients

5.5 ACCURACY CONSIDERATIONS

The accuracy of the final results is expected to be within 10 percent for the aerodynamic coefficients. Some of the aspects affecting accuracy are discussed next.

5.6 EFFECT OF THE DEFINITION OF F(Q)

As pointed out in section 4.1 the definition of F(q) is not unique. The two most relevant factors in its definition are:

i) Choice of the weight factors G_i , H_i : If these factors are set equal to unity, the discrete form of F(q) becomes:

$$F(q) = \sum_{\text{free-streamline}} \left(|\nabla\phi_i + \bar{U}_\infty| - |\bar{U}_\infty| \right)^2 \Delta\ell_i + \sum_{\text{jet}} \left(1 - \frac{|\nabla\phi_i + \bar{U}_\infty|^2}{\bar{U}_\infty^2} - \frac{\bar{C}_j}{R_i} \right)^2 \Delta\ell_i \qquad 5.5$$

If the weight factors are chosen to be the inverse of the panel length, namely $G_i = \frac{1}{\Delta\ell_i}$, $H_i = \frac{1}{\Delta\ell_i}$, the definition of F(q) becomes:

$$F(q) = \sum_{\text{free-streamline}} \left(|\nabla\phi_i + \bar{U}_\infty| - |\bar{U}_\infty| \right)^2 + \sum_{\text{jet}} \left(1 - \frac{|\nabla\phi_i + \bar{U}_\infty|^2}{U_\infty^2} - \frac{\tilde{C}_j}{R_i} \right)^2 \qquad 5.6$$

Also a combination of those alternatives can be used to define F(q).

ii) Length of the Boundary Involved: The discrete form for F(q) does not need to be calculated including for the contributions of all the panels that describe the jet or the free-streamline. Some can be omitted without substantially altering the final result. The fact that this is possible allows one to leave out panels in areas where the calculation is inaccurate, such as close to the exit of the jet. Figure 30 shows how the free-streamline and the jet enter the computation of F(q). Only the panels lying on the solid line are used.

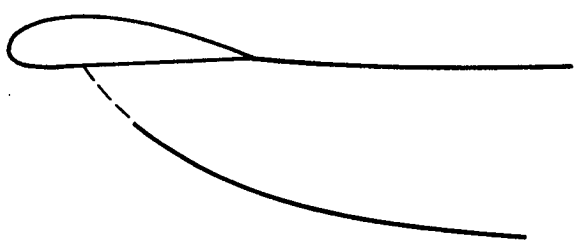

Figure 30: Part of Boundary Used in Computation of F(q)

The last 2 or 3 panels in both the free-streamline and the jet are not included in order to avoid end effects. The first few panels close to the exit of the jet are not

included for two reasons: On one hand, because, as mentioned before, the calculation of the velocities is inaccurate there, and on the other hand the scaling of the objective function is considerably improved if those panels are omitted, which allows to reach a solution with a lower number of iterations. The reason for this improvement lies in the fact that, for changes in the independent variables q which are closer to the jet exit, the corresponding changes in the curvature of the jet are much larger than the changes associated with variables far away from the jet exit.

The following table shows the typical behaviour of the aerodynamic coefficients for different definitions of F(q) and for different number of panels omitted close to the exit.

TABLE 1

Definition and Evaluation of F(q)

panels not counted	3	3	3	5	7
G_i	$1/\Delta\ell_i$	$1/\Delta\ell_i$	1	$1/\Delta\ell_i$	$1/\Delta\ell_i$
H_i	$1/\Delta\ell_i$	1	1	$1/\Delta\ell_i$	$1/\Delta\ell_i$
C_{L_i}	1.152	1.152	1.158	1.150	1.152
C_{m_i}	-0.330	-0.330	-0.332	-0.329	-0.330

5.7 EFFECT OF THE IMPLEMENTATION OF THE PANEL METHOD

The two main aspects of the panel method implementation that concern accuracy are the treatment of internal sharp corners and the density of panels.

5.7.1 Rounding of Internal Corners

As pointed out by Hess[5] if the boundary where the panels are laid out has internal sharp corners the solution is inaccurate there. In this case it was found that unrealistically high velocities are computed close to such corners. This drawback is a property of the singularity representation of the solution and cannot be eliminated by increasing the density of panels close to the corner. The standard procedure is to introduce a rounding of such corners. In the case of the airfoil-jet-freestreamline problem an internal corner exists right at the exit of the jet. A rounding is introduced as shown in Figure 31

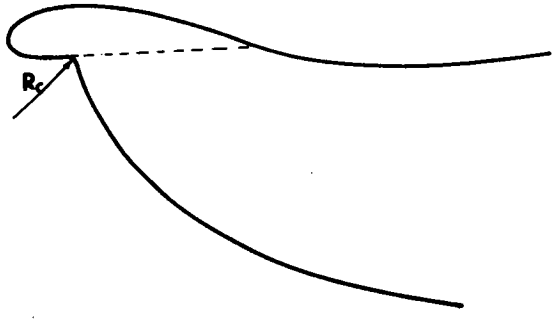

Figure 31: Rounding of Internal Corner

The effect of the sharp corner is localized and affects the shape of the wake very little. It does however affect

the aerodynamic coefficients. Figure 32 shows how the lift coefficient for a typical case varies as the radius of the rounding of the corner changes. This shows that, once the corner is slightly rounded, further increase in the radius of rounding will not affect significatly the results.

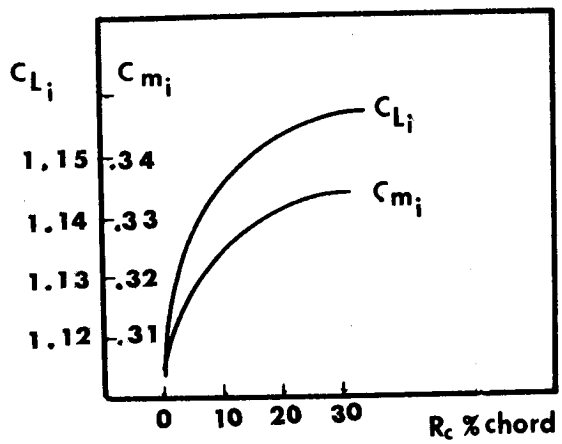

Figure 32: Effect of Radius of Rounding

5.7.2 Effect of Density of Panels

i) Density of panels in the wake area: This density affects the accuracy with which the jet and the free-streamline shapes are computed. Most of the calculations where run with about 20 panels on the jet and about 15 panels on the free-streamline. If this number is doubled, it is observed that the lift and moment coefficients undergo a change of less than 5%. Hence the density of panels used in the wake area can be considered acceptable.

ii) Density of Panels on the Airfoil: As shown in section 4.8, the aerodynamic coefficients are obtained by integrat-

ing the pressure coefficient around the airfoil, hence the density of panels on the airfoil is expected to affect the accuracy. The region where the density of panels is the most important is the nose, since it is there that the steepest gradients of pressure occur. Figure 33a shows the panelization of the airfoil nose that was used in most of the calculations. Figure 33b shows a much more dense ditribution of panels on the airfoil nose. The difference of the aerodynamic coefficients between the two cases is less than 1%.

Figure 33: Distribution of Panels on Airfoil

5.8 EFFECT OF THE JET PARAMETERS

For the sake of computational simplicity the number of independent variables q and the number of panels was kept constant in the process of the parametric study. This means that there is different accuracy between the results corresponding to different values of jet strength and jet angle. One measure of accuracy is the minimum of the objective function. The closer to zero it is, the more closely the free-streamline and the jet conditions are satisfied. Figure 34 shows such minimum for different intensities and jet

angles. The procedure is less accurate for weak shallow jets, due to the inability of the spline function to properly capture the great change of curvature in such jets.

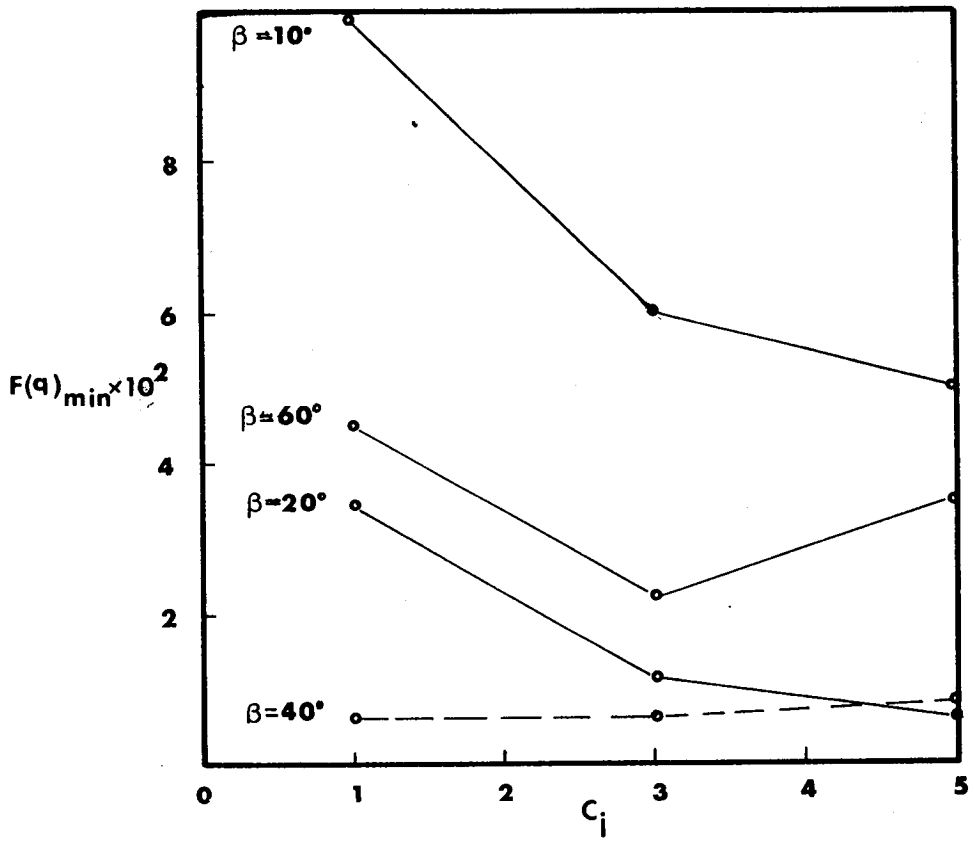

Figure 34: The Minimum of the Objective Function

Chapter VI

ANALYSIS OF THE RESULTS

In this chapter the aerodynamic properties of the airfoil with the jet are analyzed and compared with the properties of two other related systems. The analysis is carried out for the airfoil at zero angle of attack and for different values of the jet intensity, angle and location.

6.1 RELATED SYSTEMS

Figure 35 shows, in addition to the airfoil with a jet studied here, two other systems that have some characteristics in common. Those are the jet flap and the supercavitating jet-flapped hydrofoil. The linearized form of these two problems have been solved analytically[28], the linearization having been obtained assuming that the angle of ejection is small. Figure 35c shows the system object of study here when the jet is located at the trailing edge. This can also be thought of as the jet flap problem with a separation region starting at the trailing edge. Although this case would not occur in practice because the jet would prevent separation, insight in the physics can be gained by comparing these two systems. The supercavitating hydrofoil differs from the airfoil with the jet in that the free-streamline

bounding the cavity is assumed to start at the leading edge. This system has application in high speed ships, where such assumption is plausible. Its comparison with the present case will reveal remarkable similarities. In the analysis that follow a comparison between the three systems will be made.

6.2 WAKE SHAPE AND VELOCITY DISTRIBUTION

Selected wake shapes for the case of the jet at the trailing edge are shown in Figure 36 and 37. Here it is clearly seen that a relative change in the angle of the jet produces greater change in the shape of the wake and the velocity distribution that the same relative change in the strength of the jet. It is observed that, as the strength or the angle of the jet increase, both the penetration ot the jet and the departure of the free-streamline from the horizontal axis increase. This departure of the free-streamline had not been observed in Hu's calculation because of the way he estimated the position of the free-streamline. Figures 38 and 39 show similar results for the jet at 50% of the chord. It is observed that the shape of the jet and of the free-streamline are only slightly different from the case with the jet at the trailing edge, the jet trajectory just being displaced towards the leading edge by 50% of the chord.

Selected velocity distributions are shown in Figures 40, 41, 42 and 43.

6.3 AERODYNAMIC COEFFICIENTS AND CENTER OF PRESSURE

As mentioned in chapter 1, the forces acting on the airfoil as a result of the presence of the jet are caused by two different factors: asymmetric distribution of pressure and momentum ejected from the airfoil in the jet. The lift due to the pressure distribution alone will be called induced lift, denoted by C_{L_i} . The total lift coefficient is then given by

$$C_L = C_{L_i} + \frac{\tilde{C}_j}{c} \sin\theta$$

where θ is the angle formed by the jet at the point of exit with the direction of the free-stream.

6.3.1 Jet at 100 % of the Chord

In Figure 44 it is shown how the induced lift coefficient varies as a function of the jet strength for different values of the jet angle. Figure 45 compares the induced lift with the induced lift produced by the jet flap. The difference between the two can be viewed as the loss that a jet flap system would suffer due to the presence of a wake starting at the trailing edge. Such a loss is quite considerable, being of the order of 2/3 of the jet flap induced lift.

Figure 46 shows the total lift coefficient as function of the jet angle, for different jet strengths. This Figure shows a remarkably linear relation, even for rather large angles of the jet.

The position of the center of pressure, which is defined as the point of intersection between the resultant force acting on the airfoil and the chord, is sketched in Figure 47 as a function of the jet intensity for two very different values of the jet angle. It is seen that the jet angle has very little effect on the location of the center of pressure. In the linearized analysis of the jet flap and the supercavitating jet-flapped hydrofoil the position of the center of pressure turns out to be strictly independent of the jet angle. The center of pressure for the airfoil with the jet, calculated at a representative angle $\beta = 40$ is compared with the center of pressure of the jet flap in Figure 48. As the strength of the jet increases, the center of pressure in the airfoil with a jet moves towards the trailing edge much more quickly than in the case of the jet flap.

6.3.2 Jet at Other Locations on the Chord

The change undergone by the induced lift as the jet is moved to different chord locations is shown in Figure 49. The most important fact about this result is that the relative change in induced lift as the jet position changes is

rather small, and for shallow jets it is almost negligible. This means that the total lift is very weakly affected by the jet location. Regarding the position of the center of pressure, the characteristics observed in the previous subsection still exist for the jet at different locations. This is shown in Figure 50. When the jet is located at the quarter of the chord the position of the center of pressure remains almost independent of the jet strength and angle.

6.4 EFFECTIVENESS OF THE JET

A measure of the capability of the jet to produce lift is given by $\frac{\partial C_L}{\partial \beta}$, called jet effectiveness. Figure 51 shows the effectiveness of the jet for the three related systems. The present case, for a shallow jet is very close to the supercavitating hydrofoil in this respect, the jet in the jet flap system, on the other hand, is much more effective than the jets in the other two systems. In view of what was pointed out in the previous section, the effectiveness of the jet will be almost independent of the jet location along the chord. Figure 52 shows how the derivative of the moment coefficient with respect to the jet angle varies for different jet intensities and jet locations. Once again, a close similarity with the supercavitating hydrofoil exists.

6.5 LINEARITY

In a linearized analysis of the airfoil-jet-freestream-line problem the penetration of the jet and the departure of the free-streamline from the plane of the airfoil would be considered to be linear functions of a suitably chosen small parameter. The obvious parameter in this case would be the jet angle, which was used to obtain the linearized expressions for the jet flap and the supercavitating hydrofoil. The results of the present study, which account for non-linear effects, can be used to asses to what extent a linearized analysis would capture the physics of the problem. A strong suggestion that a linear analysis would be successful has already been indicated by the linearity in the jet angle pointed out in the previous sections. Figure 53 shows how the jet penetration and the free-streamline departure depend on the jet angle. This values are taken at fixed location on the wake. This linearity strongly suggests that a linear analysis will be successful even for large angles of the jet, as it was the case in the jet flap analysis.

Chapter VII

CONCLUSIONS AND RECOMENDATIONS

7.1 CONCLUSIONS

7.1.1 Physics Revealed by the Inviscid Model

i) The use of the inviscid model described in chapter 1 leads to results that have some similarity to results obtained by the use of linear theories for the jet flap and supercavitating jet-flapped hydrofoil problems. The two more important such similarities are the linear dependence of the geometry and aerodynamic coefficients on the angle of the jet, and the fact that the location of the center of pressure is almost independent of the jet angle, and a function of the jet intensity only.

ii) The lift is almost independent of the position of the jet exit on the chord. As the jet is moved forward the decrease in the decrease of the high pressure region on the lower surface of the airfoil is almost balanced by the increase of suction on the upper surface, close to the nose, in a way that the resultant lift coefficient remains almost constant.

7.1.2 Characteristics of the Method of Solution

i) Improvement over previous method: Aside from being much more flexible, the present method computes the unknown parts of the boundary as a whole, as opposed to the method in Reference 1 where the jet and the free-streamline are dealt with separately.

ii) Flexibility: the method developed here requires little or no outside intervention in the process of computation and is relatively easy to implement. The method constitutes also a general procedure for the solution of a type of boundary value problems in which the position of the boundary is not known a priory. Although entrainment was not included in the model used here, the method will in principle be able to handle a model for entrainement which would involve just a modification of the boundary conditions on the jet.

iii) Expensive in its present form: since nothing else but the value of the objective function is provided to the optimization algorithm, and the objective function is expensive to evaluate, the method is in general rather costly in its present form.

7.2 RECOMENDATIONS

7.2.1 The Physical Problem

Very little experimental data are available on this lifting system, and much more is needed to understand some of the most important aspects. Such is the case of the wake bounded by the airfoil and the jet, and the entrainment process. A clear picture of what happens in the wake is essential if a more realistic model is to be constructed, and an understanding of how the entrainment process occurs would be needed to model the entrainment in some simple form. Precisely because of the importance of these factors, the results given here are only expected to give qualitative agreament with experiments.

7.2.2 The Mathematical Model

In order to better understand the mathematical model the following aspects can be considered:

i) Modification to Include Entrainment: this modifications consist in changing the boundary conditions in a way that the additional velocity field produced by entrainment is accounted for.

ii) Analysis of the Linearized Solution: the potential usefulness of the linearized approach is one of the conclusions

of the non-linear study done here. A linearized approach would allow one to investigate the bahaviour of the system for very small values of jet strength and jet angle, which are aspects that the this study fails to capture.

iii) Further Analysis of Related Problems: A whole family of airfoil-jet-freestreamline problems could be considered, in which both the position of the jet and the position of the separation point of the free-streamline are varied along the airfoil, as opposed to just varying the position of the jet. Such a family of problems is likely to have interesting aerodynamic properties.

7.2.3 Improvements on The Method of Solution

In order to lower the cost of the method and improve the accuracy, the following steps are suggested, all of which constitute substantial areas of research:

i) Scaling Improvement: This aspect will affect the cost. Scaling is a subject of great concern in non-linear programming, and substantial research is being invested in the development of algorithms capable of changing the scaling as the calculation proceeds.

ii) Increase Information on Objective Function: This aspect will also affect the cost. The next most important piece of

information of a function next to the value of the function itself is its gradient. If a way of computing the gradient of F(q) is developed which does not consist of a straight application of finite differences as it is done in the present code, a substantial amount of computational time can be saved. The developement of such a way of computing the gradient would imply to exploit the fact that a very small change in the independent variables q produces a change in the imbalance of the jet condition and the free-streamline condition which is to some extent localized in an area of the boundary.

iii) Include "C" Part of the Boundary: As discussed in section 3.1 this part of the boundary was ignored on the assumption that if the wake is long enough it is still possible to obtain an approximate solution with a truncated wake. Including the "C" part of the boundary will affect the accuracy and would allow one to work with a much shorter wake, permitting a very accurate resolution of the wake shape.

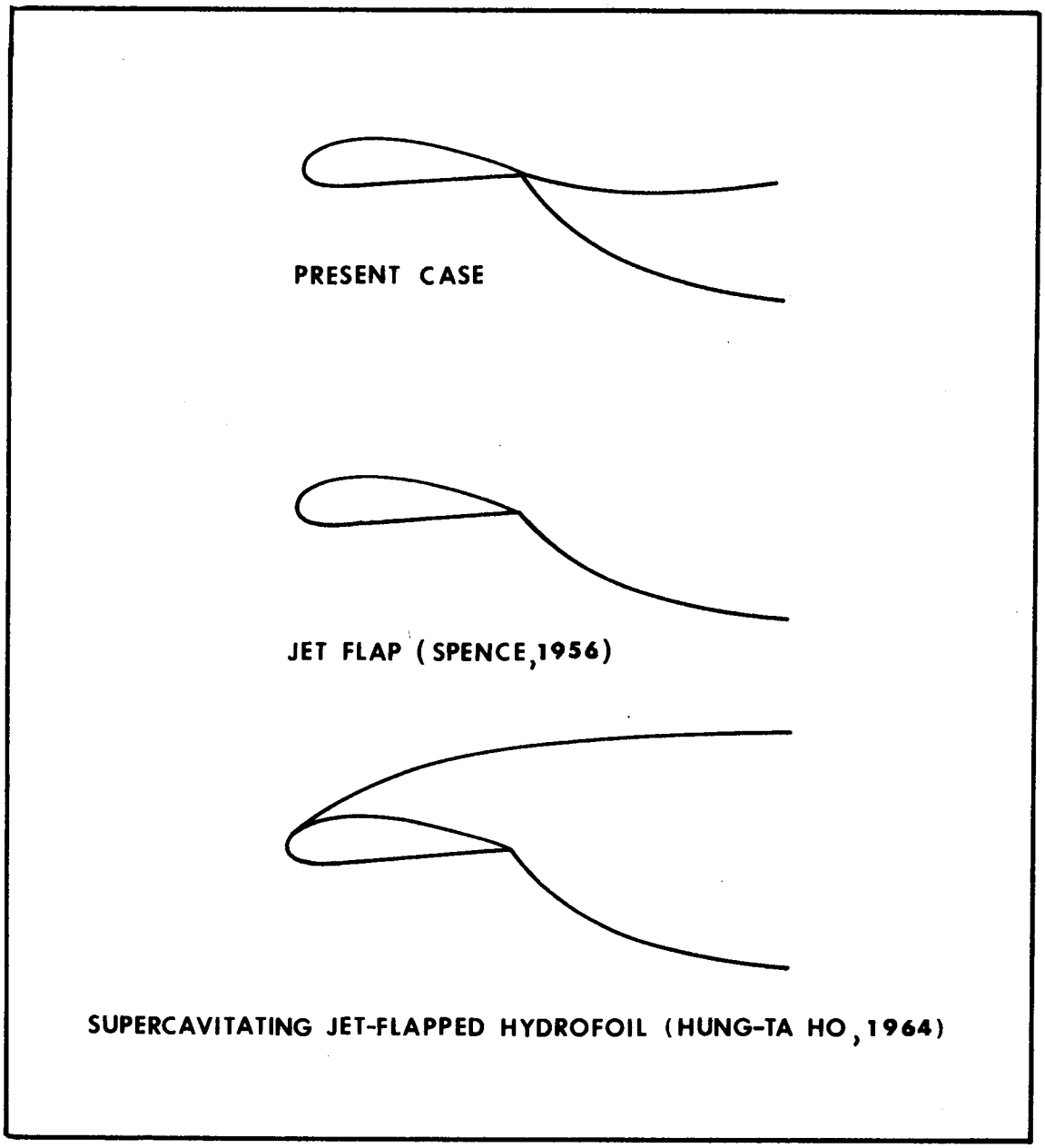

Figure 35: Related Systems

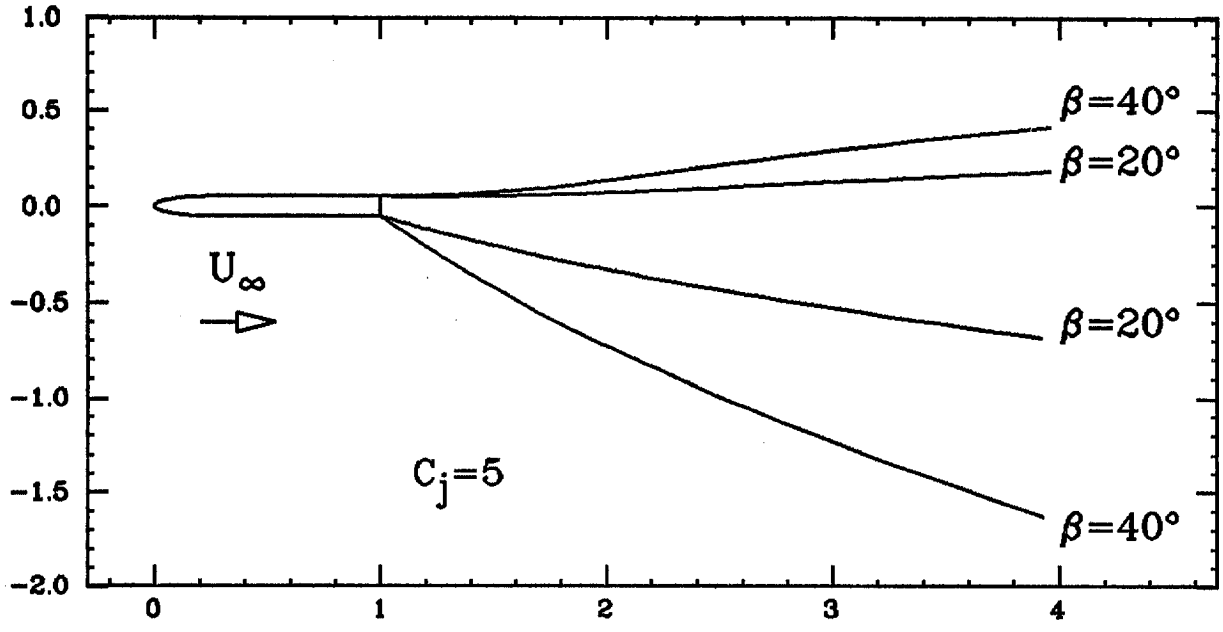

Figure 36: Wake Geometry, Jet at 100% of the Chord

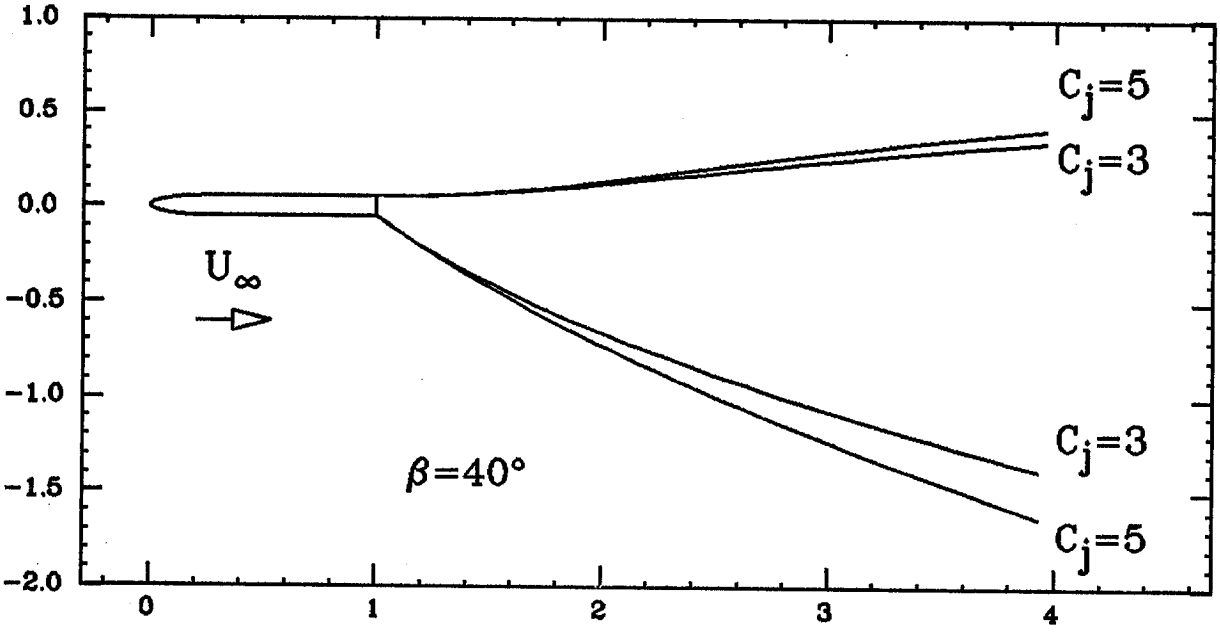

Figure 37: Wake Geometry, Jet at 100% of the Chord

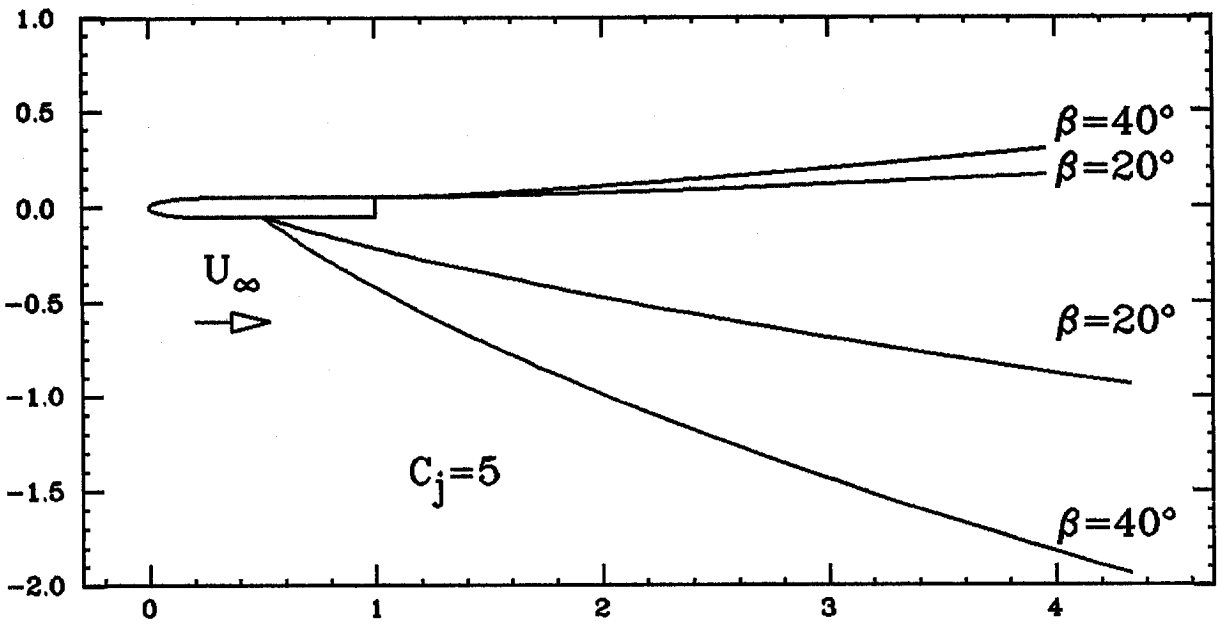

Figure 38: Wake Geometry, Jet at 50% of the Chord

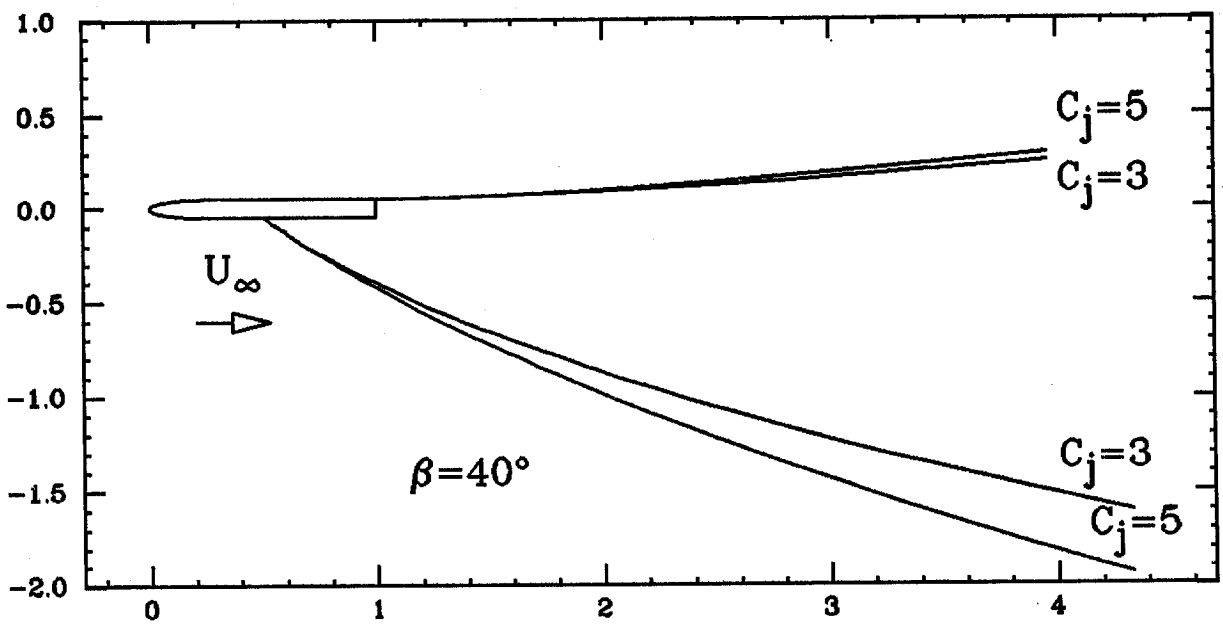

Figure 39: Wake Geometry, Jet at 50% of the Chord

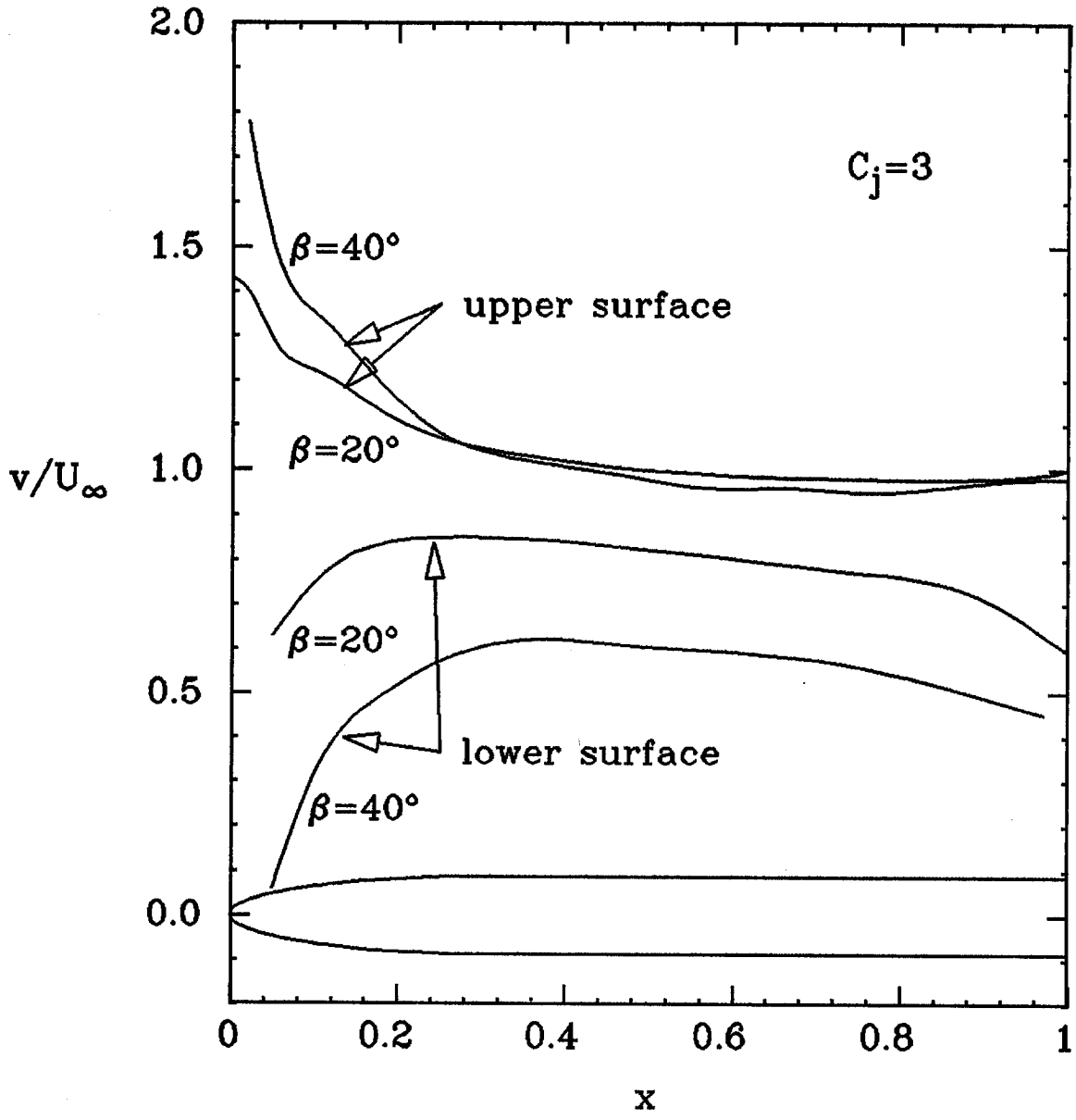

Figure 40: Velocity Distribution, Jet at 100% of the Chord

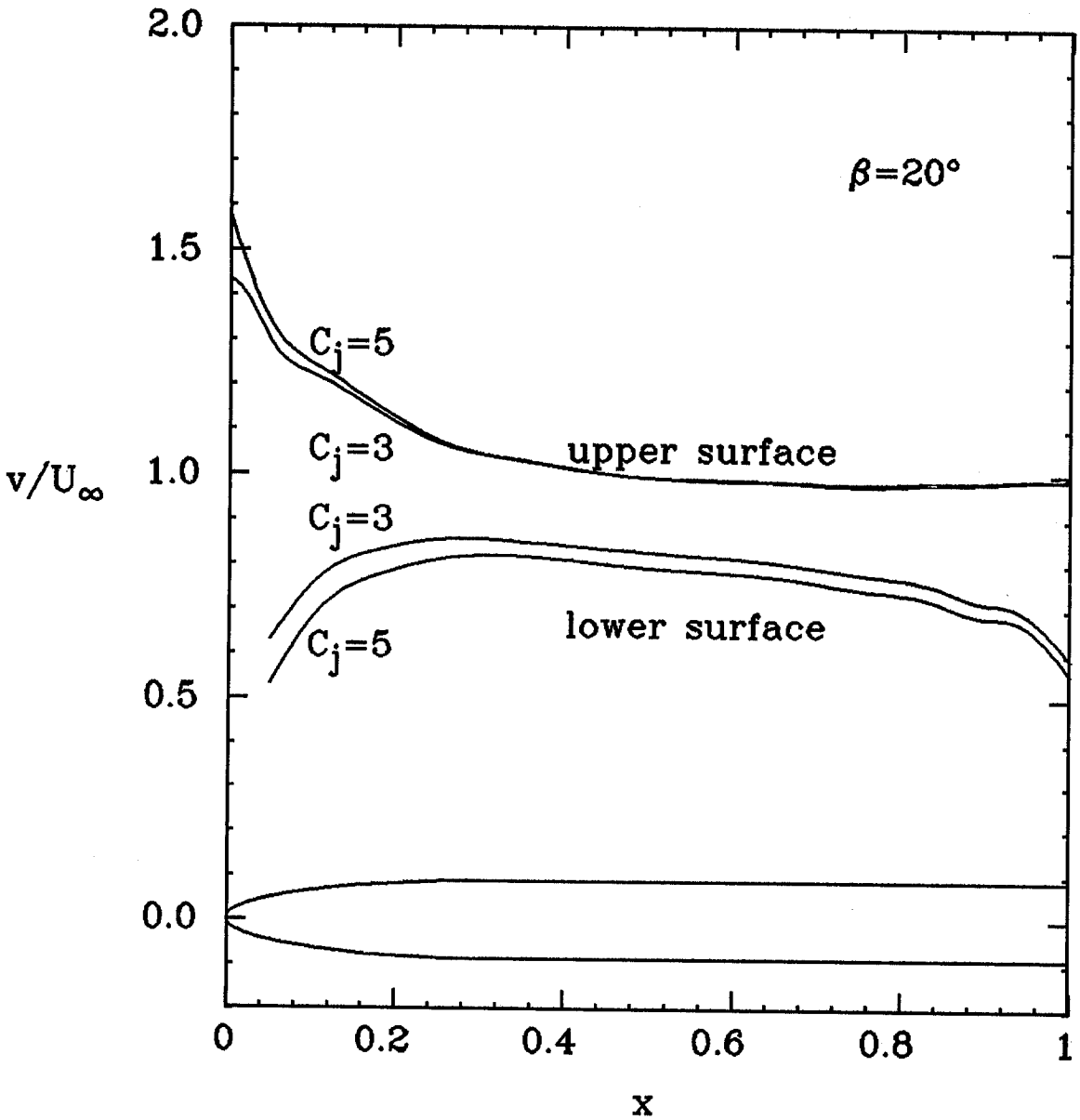

Figure 41: Velocity Distribution, Jet at 100% of the Chord

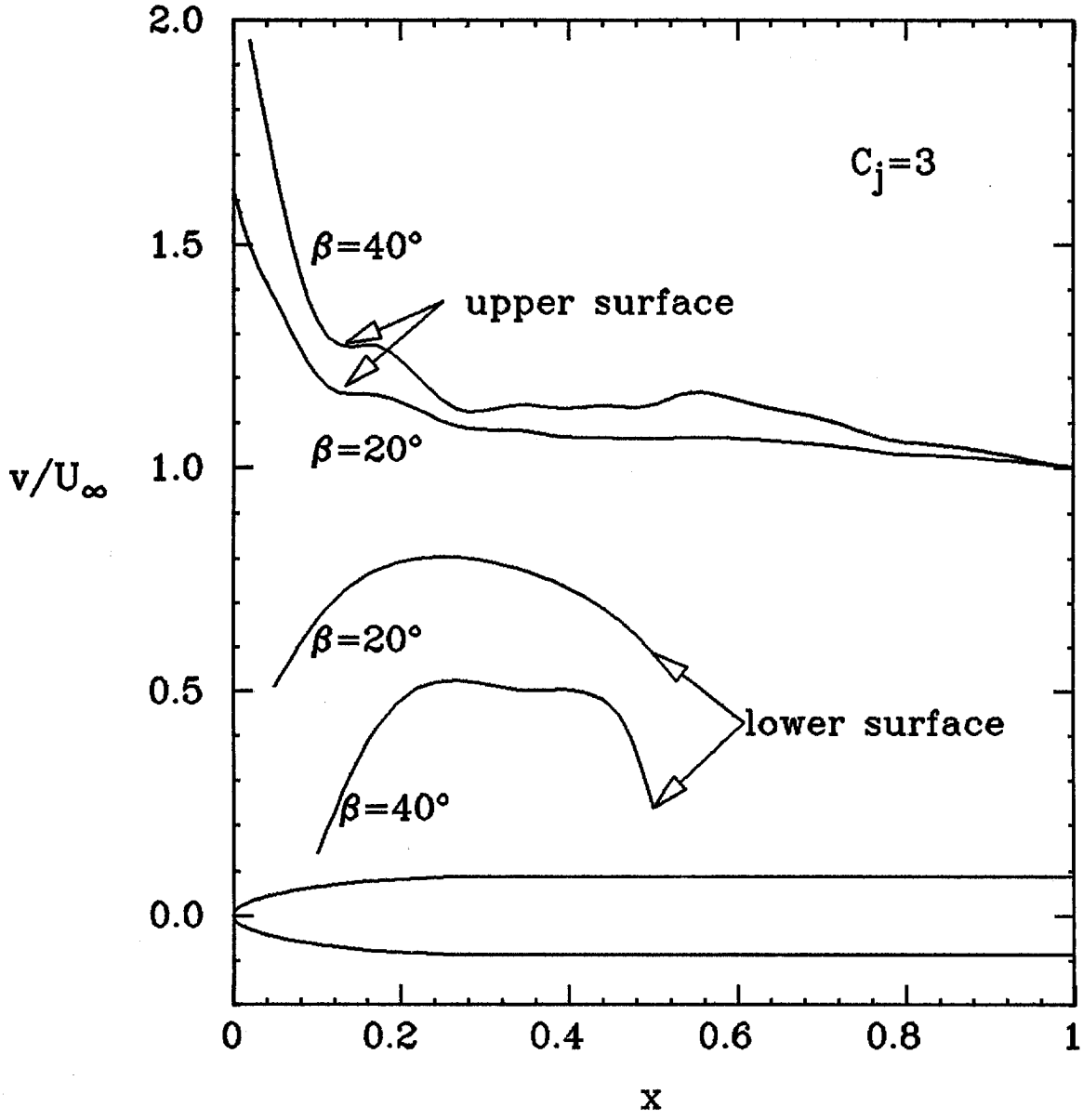

Figure 42: Velocity Distribution, Jet at 50% of the Chord

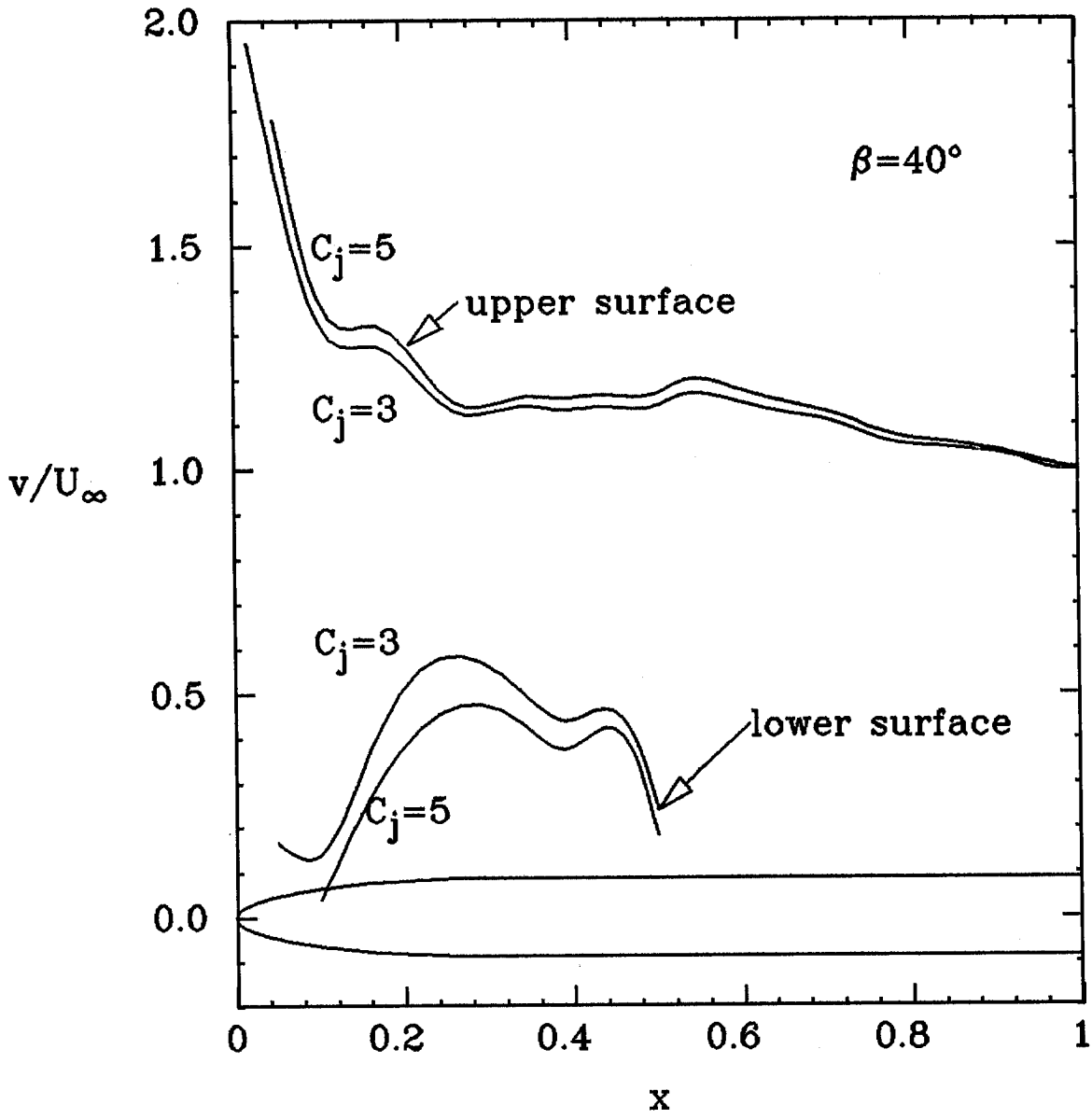

Figure 43: Velocity Distribution, Jet at 50% of the Chord

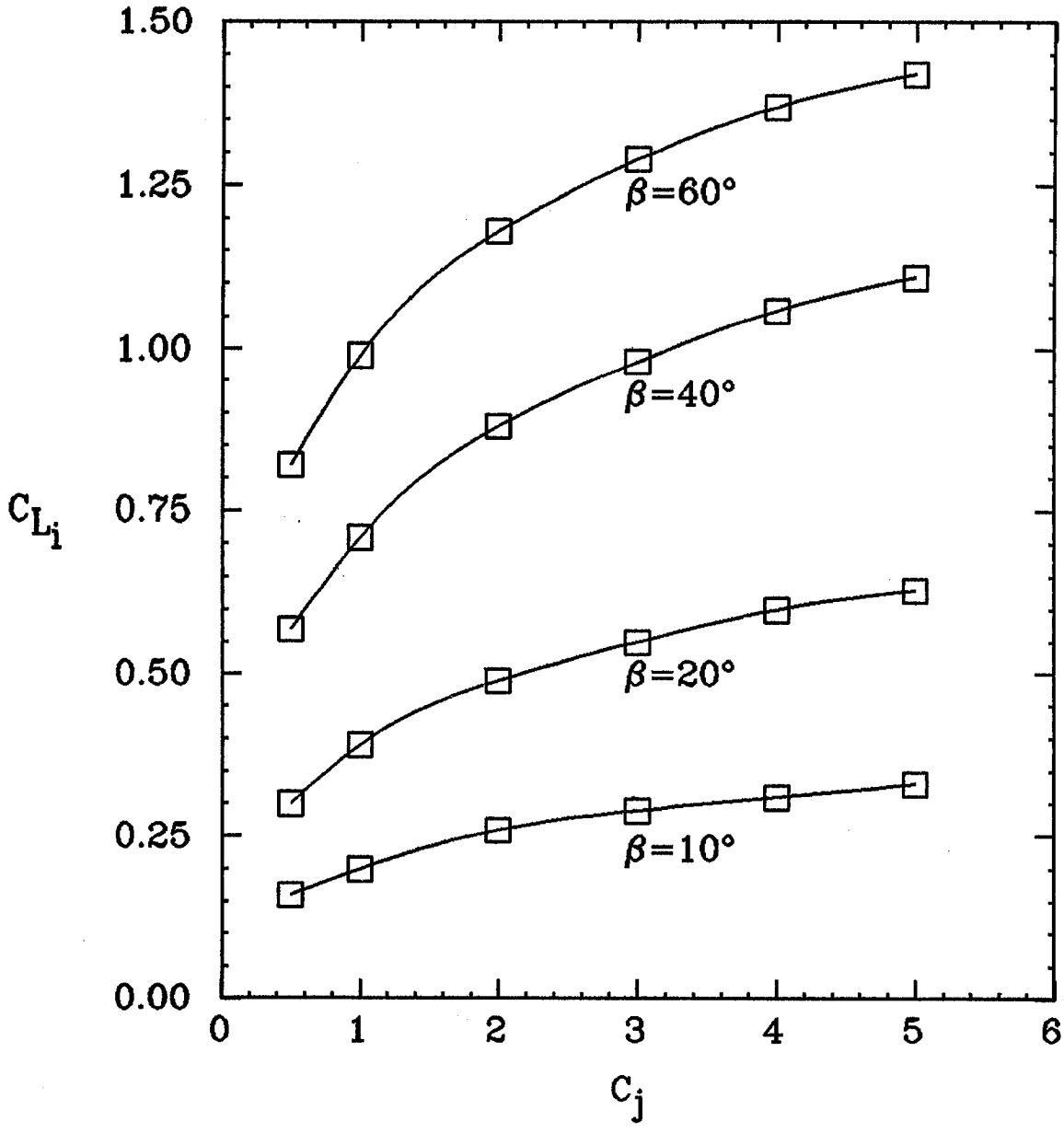

Figure 44: Induced Lift

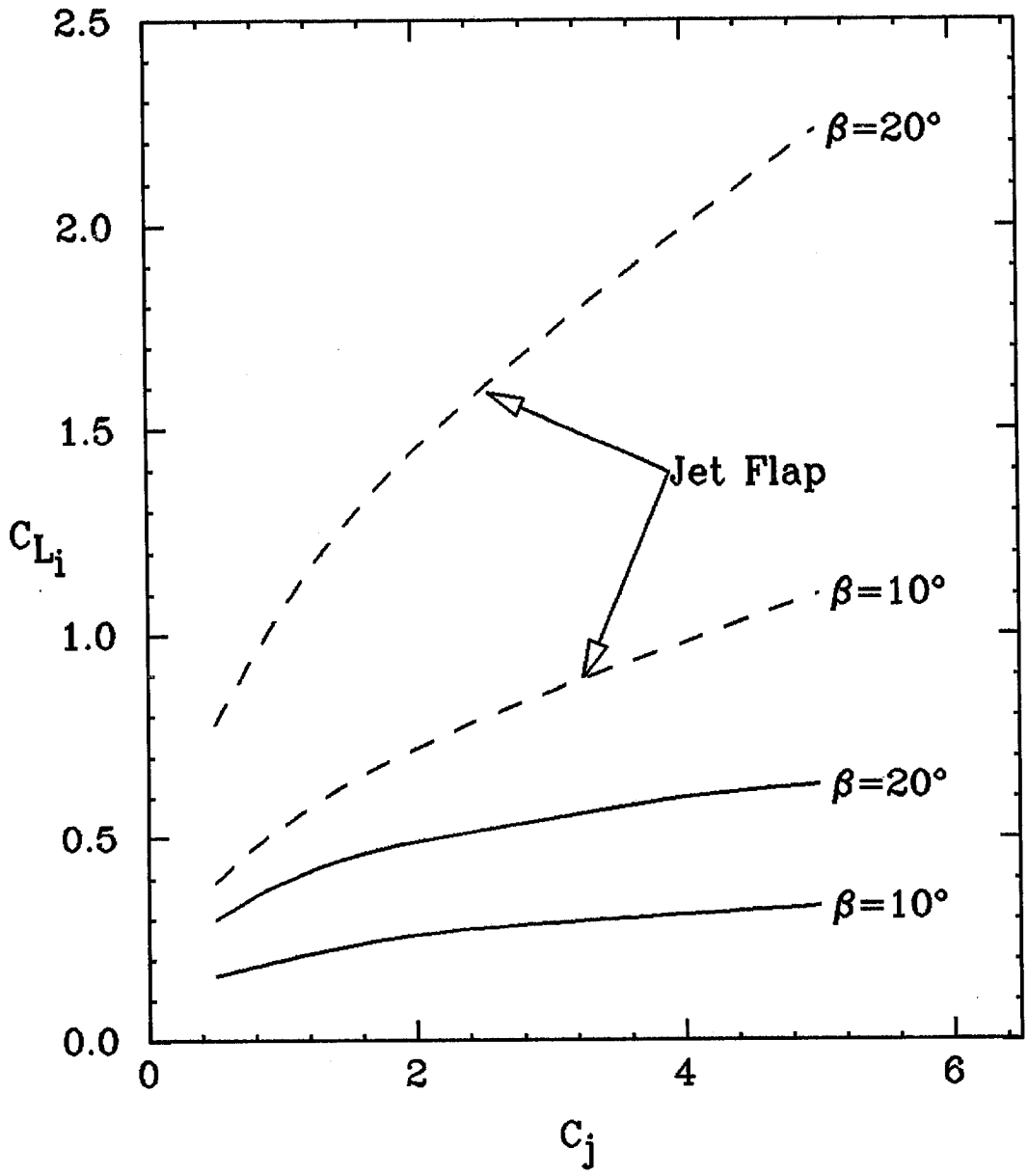

Figure 45: Comparison with the Jet Flap

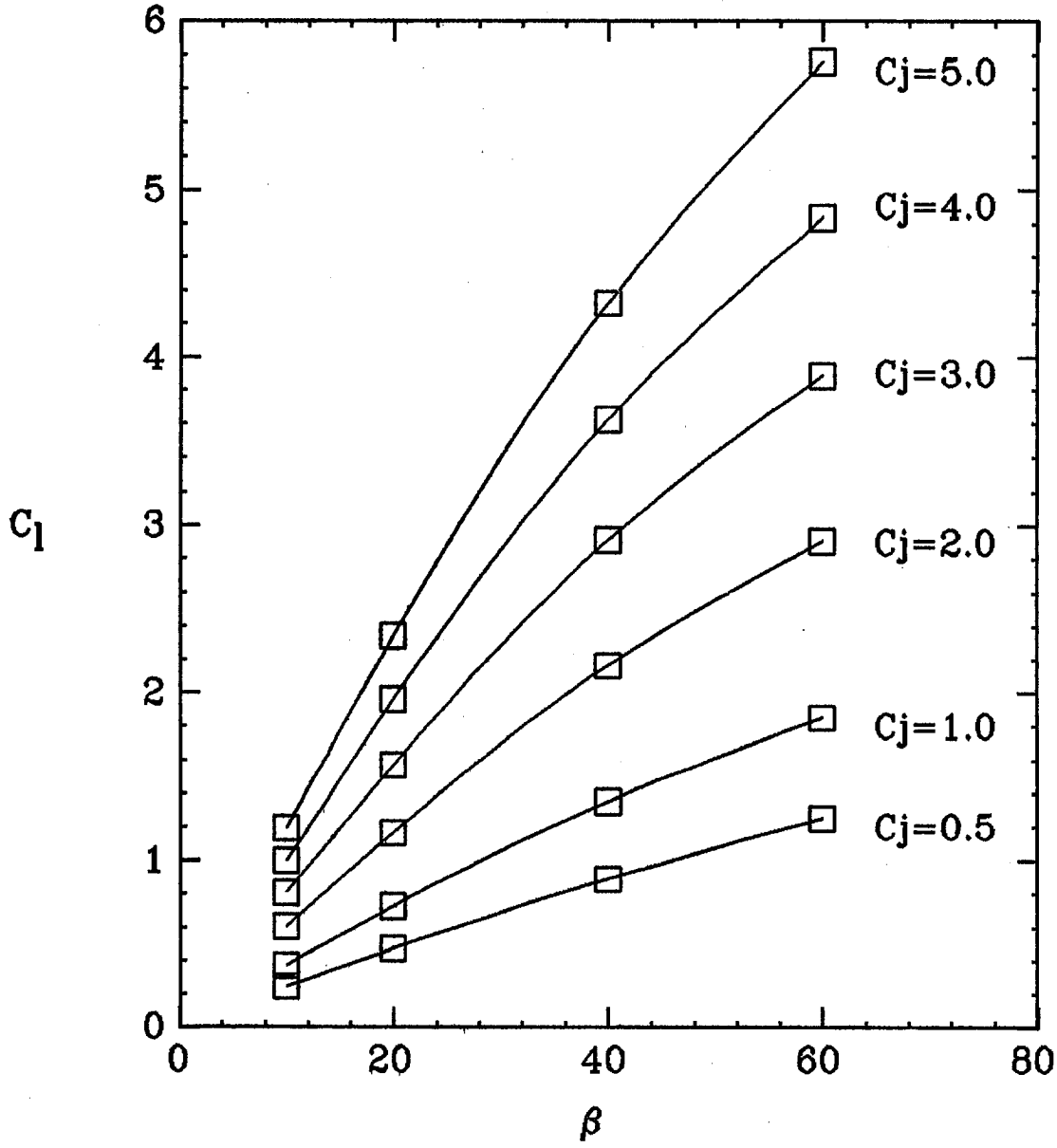

Figure 46: Total Lift

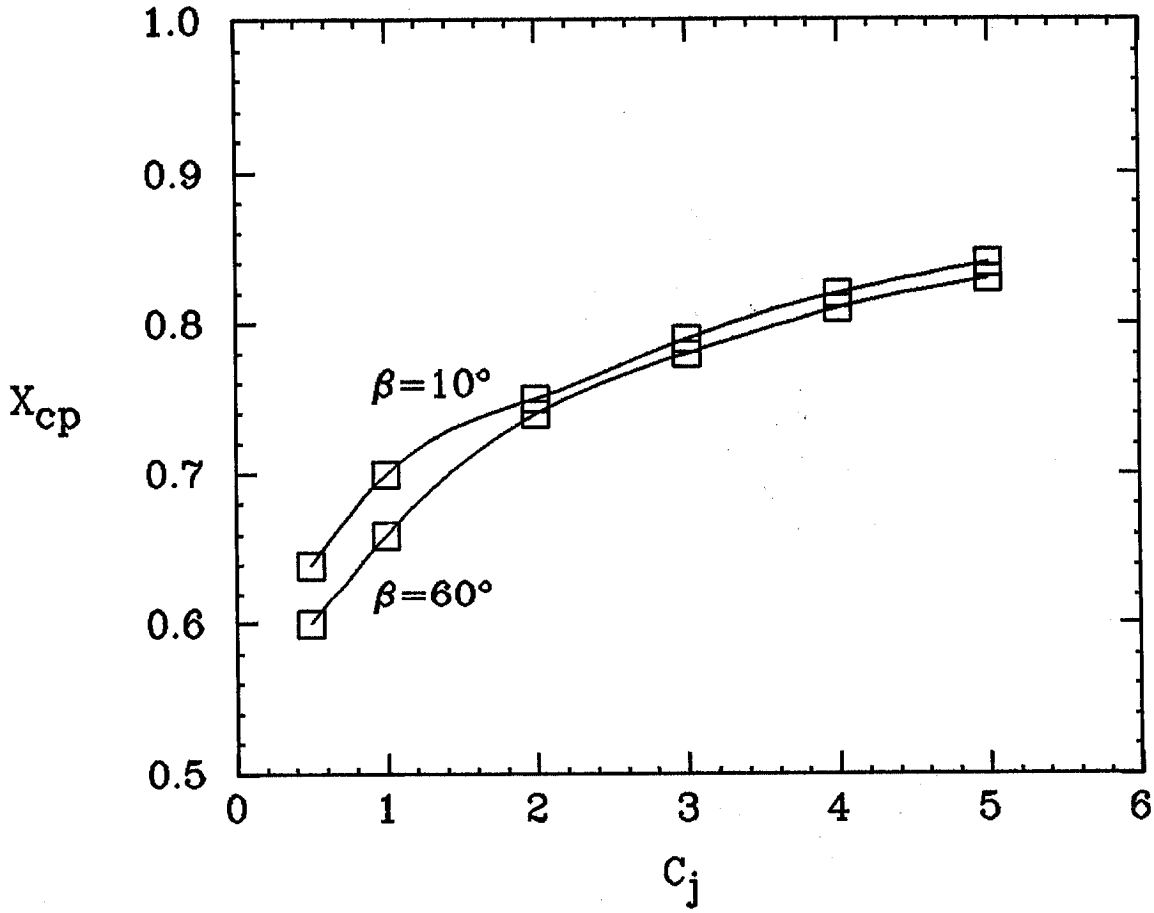

Figure 47: Center of Pressure

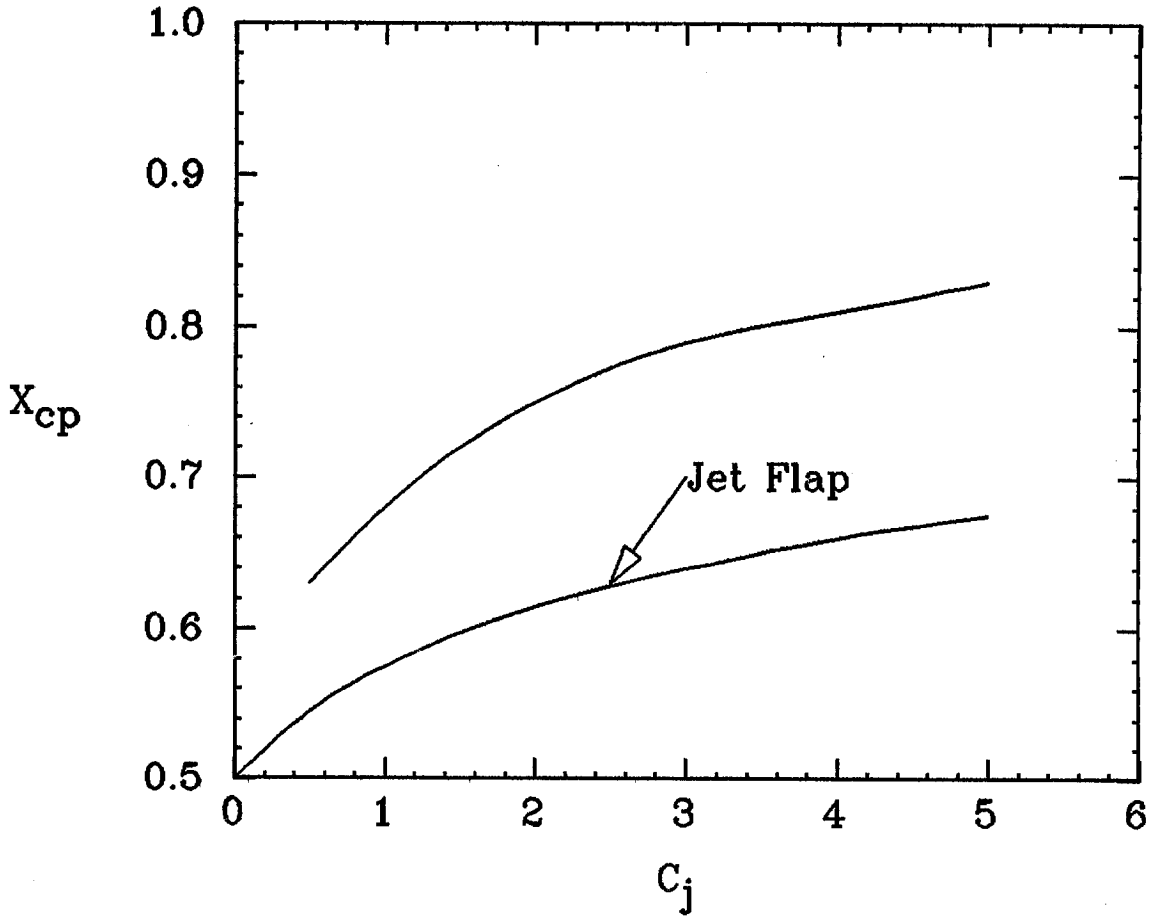

Figure 48: Comparison with the Jet Flap

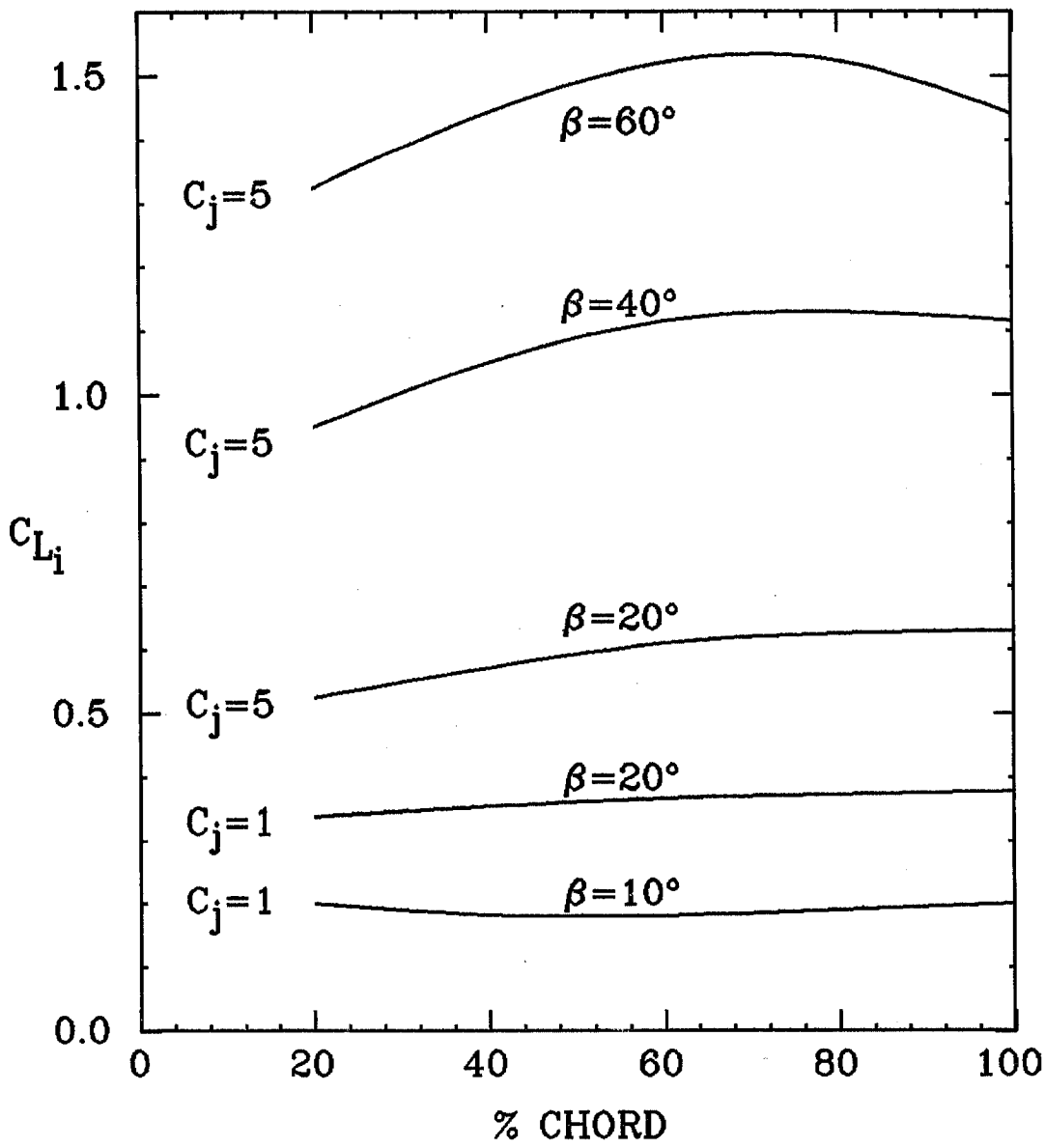

Figure 49: Effect of the Jet Position on the Lift

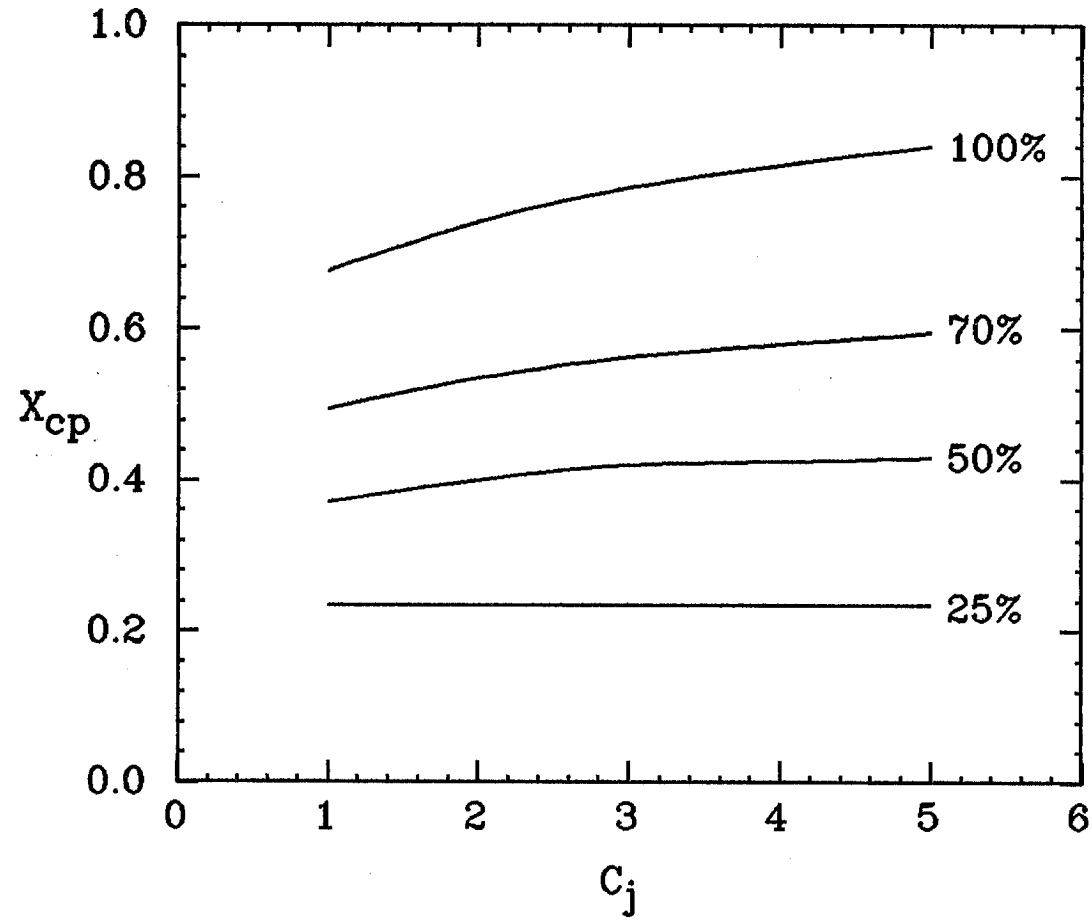

Figure 50: Effect of the Jet Position on the Center of Pressure

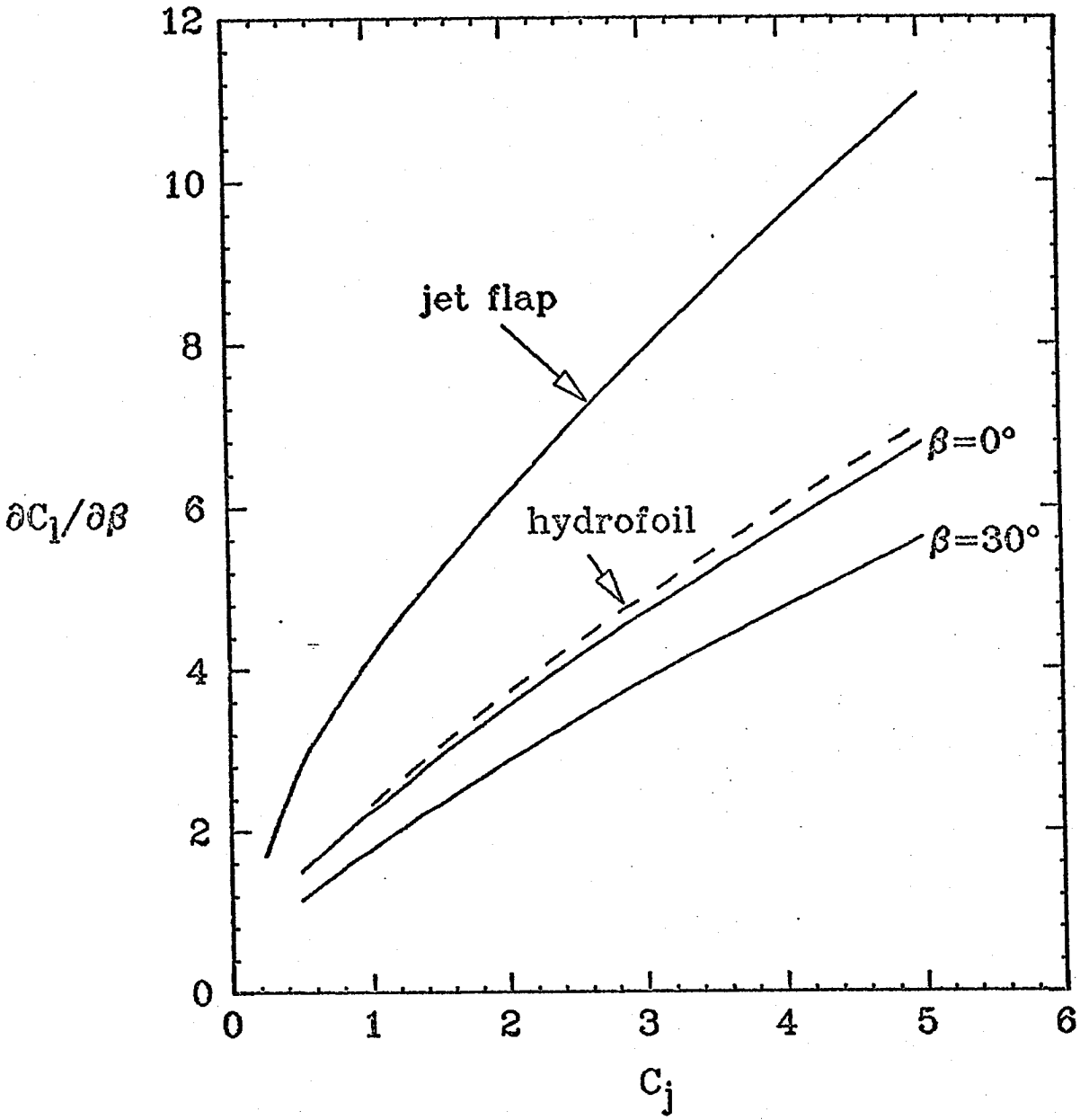

Figure 51: Jet Effectiveness

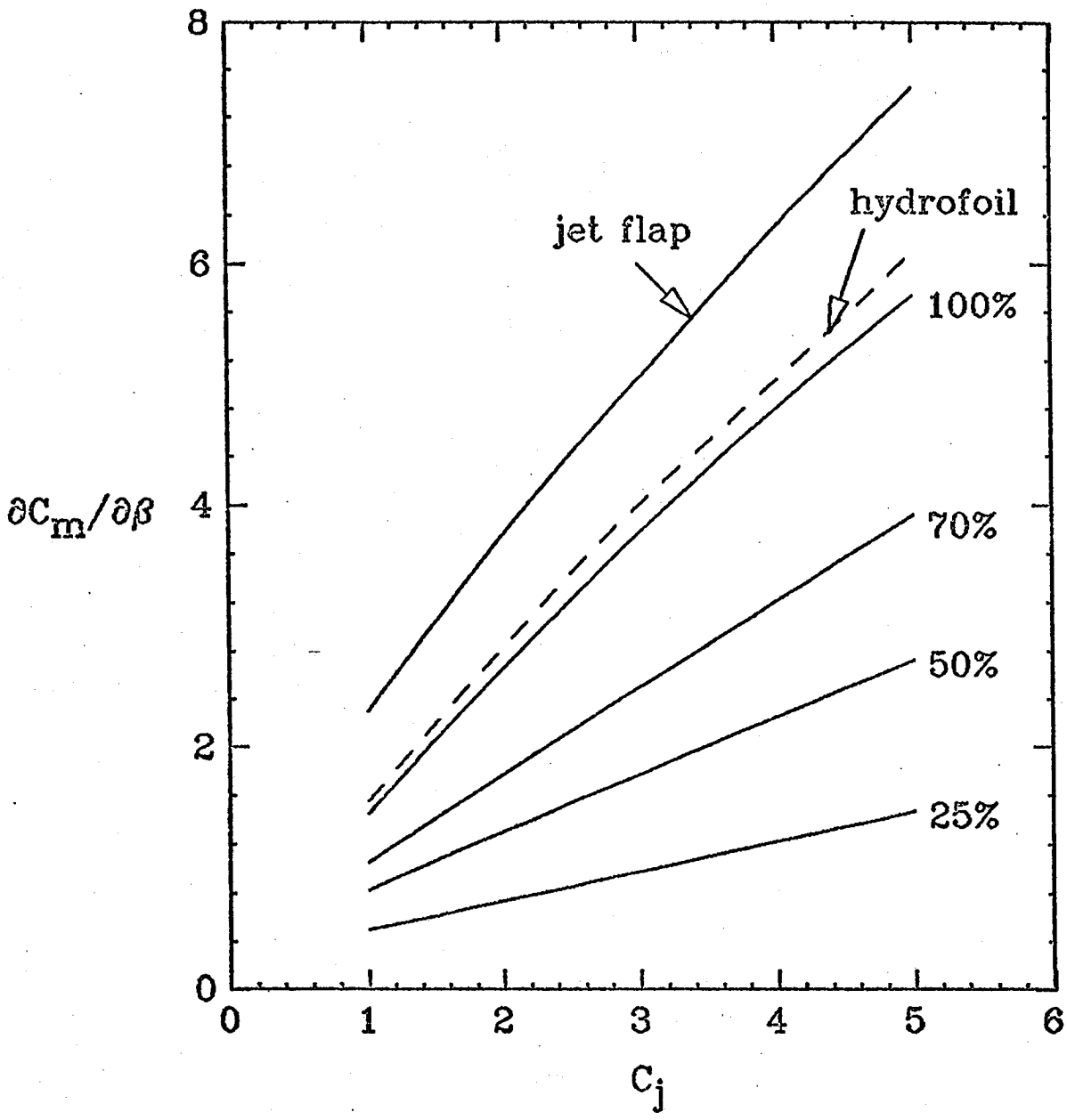

Figure 52: Moment Derivative

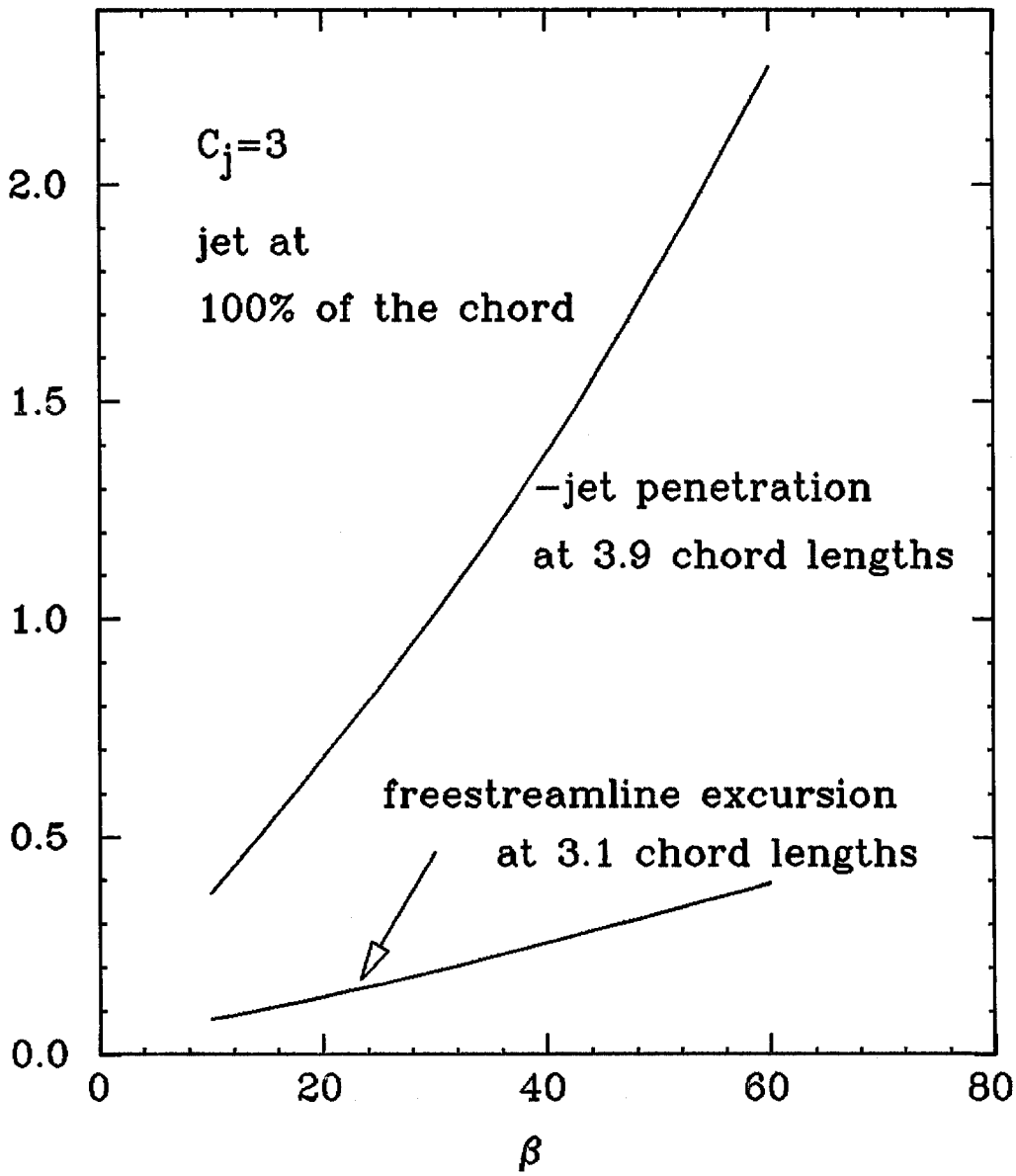

Figure 53: Wake Widening

REFERENCES

Hu, G. An Analysis of a Two-Dimensional Propulsion Wing Ph.D. thesis, Stanford University, 1971.

Spence, D. A. The Lift Coefficient of a Thin, Jet-flapped Wing Proc. Roy. Soc. Series A, Vol. 238, No. 121, 1956.

Birkhoff, G. and Zarantonello, E. N. Jets, Wakes and Cavities Academic Press, N.Y. 1957.

Ahlberg, J. R., Nilson, E. N. and Walsh, J. L. The Theory of Splines and Their Applications Academic Press, N.Y. 1967.

Hess, J. L. and Smith A. M. O. Calculation of Potential Flows about Arbitrary Bodies Prog. in Aer. Sc., Vol. 8, Pergamon Press, N.Y. 1966.

Gill, M. and Pitfield The Implementation of the Revised Quasi-Newton Algorithms for Unconstrained Optimization National Physical Laboratory, Division of Numerical Analysis and Computing, Report No. DAC 11, 1972.

Ackerberg, R. C. On a Non-linear Theory of Thin Jets, Part I J. Fluid Mech., Vol. 31, Part 3, 1968.

Hung-Ta, H. The Linearized Theory of a Supercavitating Hydrofoil with a Jet Flap ASME, paper 64-FE-7, 1964.